

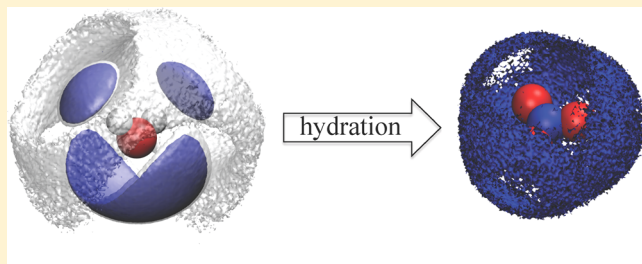
NO₃⁻ Coordination in Aqueous Solutions by ¹⁵N/¹⁴N and ¹⁸O/^{nat}O Isotopic Substitution: What Can We Learn from Molecular Simulation?

Ariel A. Chialvo*[†] and Lukas Vlcek^{†,‡}

[†]Chemical Sciences Division, Geochemistry and Interfacial Sciences Group, Oak Ridge National Laboratory, Oak Ridge, Tennessee 37831-6110, United States

[‡]Joint Institute for Computational Sciences, Oak Ridge National Laboratory, Oak Ridge, Tennessee 37831-6173, United States

ABSTRACT: We explore the deconvolution of water–nitrate correlations by the first-order difference approach involving neutron diffraction of heavy- and null-aqueous solutions of KNO₃ under ¹⁴N/¹⁵N and ^{nat}O_N/¹⁸O_N substitutions to achieve a full characterization of the first water coordination around the nitrate ion. For that purpose we performed isobaric-isothermal simulations of 3.5 m KNO₃ aqueous solutions at ambient conditions to generate the relevant radial distribution functions required in the analysis (a) to identify the individual partial contributions to the total neutron-weighted distribution function, (b) to isolate and assess the contribution of NO₃⁻…K⁺ pair formation, (c) to test the accuracy of the neutron diffraction with isotope substitution based coordination calculations and X-ray diffraction based assumptions, and (d) to describe the water coordination around both the nitrogen and oxygen sites of the nitrate ion.



1. INTRODUCTION

The hydration behavior (speciation) of nitrate ion in aqueous solution is of central interest in the development of potential selective extractants for nitrate ion in technological applications, and in understanding its reactivity and eventual fate in natural (*e.g.*, groundwater) environments.^{1,2} Consequently, it has been the target of numerous experimental studies involving X-ray,^{3–16} neutron diffraction,^{17–22} nuclear magnetic resonance (NMR),^{23–29} Raman,^{6,7,11,13–15,23,30–34} and infrared (IR) spectroscopies.^{35–41} The experimental effort has been complemented by theory and modeling involving quantum and *ab initio* methods,^{42–50} as well as molecular simulations^{22,51–60} to aid the elucidation of the aqueous environment around the anion, its dynamics, and the effect of the nature of the counterion.

Because nitrates exhibit weaker interactions with water than water with itself, these anions induce little distortion of the hydrogen bonding of the surrounding water to the extent that it has frequently been assumed that the water environments beyond the first water-oxygen coordination is uniformly distributed.^{4,6} In fact, compared to smaller monovalent or divalent ions, nitrates are weakly hydrated as a result of their small charge and relatively large effective ionic radius, *i.e.*, low charge density.⁶¹ An effective measure of the strength of such interactions is given by the ion–water first coordination numbers for the nitrogen and the oxygen sites of the nitrate ion, formally given by $n_N^{X_w}(r_u) = 4\pi\rho_{X_w}\int_0^{r_u} g_{X_w N}(r)r^2 dr$ and $n_{O_N}^{X_w}(r_u) = 4\pi\rho_{X_w}\int_0^{r_u} g_{O_N X_w}(r)r^2 dr$, where X_w denotes the oxygen or hydrogen site of water, g_{xy}(r) is the radial distribution

function (RDF) for the x…y pair interactions, ρ_{X_w} is the number density of the X_w species, and r_u indicates the radius of the coordination shell (typically described by the location of the first valley of g_{xy}(r)). However, except for molecular simulation, neutron diffraction with isotope substitution (NDIS), and (to some extent) X-ray diffraction (XRD) approaches that explicitly involve microstructural input, other existing techniques provide coordination information based on indirect or conjectured connections whose immediate result is a great disparity in the reported coordination data. For example, on the one hand, NMR^{25,26} and IR³⁷ measurements resulted in coordination numbers at odds with one another, *i.e.*, 0.5, 6, and 3.7, respectively. On the other hand, earlier XRD from Caminiti et al. provided coordination number $n[NO_3^- \cdots H_2O] \sim 6^3$ and $n_{N-H_2O} = 8.8 \pm 0.6^6$ according to their own notation, while NDIS from Neilson and Enderby¹⁷ resulted in $n_N^{O_w} \sim 1.3$ coordinating water molecules around the nitrate's nitrogen site.

These contrasting outcomes highlight unresolved issues regarding the extraction and interpretation of the hydration microstructure of the nitrate ion in a variety of aqueous environments. One relevant issue involves the effect of the cation's identity and the salt concentration on the potential ion-pair formation whose contribution to the resulting structure must be identified and isolated for the proper counting of the coordinating water molecules. This issue became evident in

Received: October 14, 2014

Revised: December 16, 2014

Published: December 16, 2014

recent XRD experiments on aqueous $\text{Ca}(\text{NO}_3)_2$ by Smirnov et al.¹⁰ who found $n[\text{N}\cdots\text{H}_2\text{O}] \sim 7.7 \pm 0.3$ and $n[\text{N}\cdots\text{H}_2\text{O}] \sim 6.9 \pm 0.3$ as the nitrate concentration decreased from 12 to 7.3 M at ambient conditions, as well as those from Levochkin et al.¹² involving $\text{Co}(\text{NO}_3)_2$ at increasing dilution that revealed the significant increase in the coordination of the nitrate ion, from $n[\text{N}\cdots\text{H}_2\text{O}] \sim 3.0$ (at 1:15 mol ratio and ambient conditions) to $n[\text{N}\cdots\text{H}_2\text{O}] \sim 9.0$ water molecules (at 1:40 mole ratio and ambient conditions), where the observed variation in coordination was interpreted as a decrease of ion pairs in favor of fully hydrated ions.

A second issue regards the overlap of several inter- and intraatomic correlations within the same radial distance where we expect the occurrence of the $\text{NO}_3^- \cdots \text{H}_2\text{O}$ correlations, *i.e.*, the $2.0 < r (\text{\AA}) < 4.4$ range. This overlapping behavior, caused by the weak hydrogen scattering, hinders not only the XRD determination of the water orientation around the nitrate ion but also the interpretation of the coordinating environment from heavy-water NDIS. In fact the experiments involving $^{14}\text{N}/^{15}\text{N}$ substitution in aqueous NaNO_3 solutions revealed strong hydrogen bonding (*i.e.*, $\text{D}\cdots\text{N}$ interactions at $r_{\text{ND}} \sim 2 \text{\AA}$),¹⁷ while similar experiments on aqueous NaNO_3 and ND_4NO_3 ^{18–20} exhibited no prominent hydrogen-bonding peaks.

Finally, a third issue concerns the presence of intraatomic correlations that might become handy physical constraints to check the proper normalization of the radial (neutron or X-ray) weighted distribution functions, with direct impact on the accuracy of the calculated coordination quantities from diffraction experiments.

Given this state of affairs in the determination of nitrate hydration behavior, here we suggest an alternative approach based on the interplay between NDIS ($^{14}\text{N}/^{15}\text{N}$ and $^{\text{nat}}\text{O}_{\text{N}}/^{18}\text{O}_{\text{N}}$) experiments and molecular simulations of aqueous nitrates as an effective tool to gain crucial insight into the microstructure of the nitrate hydration shell. The novelty behind the proposed methodology is 2-fold: (a) it takes advantage of the newest findings regarding the scattering-length contrast between ^{18}O and $^{\text{nat}}\text{O}$, *i.e.*, $0.204 \pm 0.003 \text{ fm}$ ⁶²—*i.e.*, nearly a factor of 6 greater than the earlier tabulated value⁶³—making feasible NDIS experiments using $^{\text{nat}}\text{O}/^{18}\text{O}$ substitution,⁶⁴ and (b) it involves the use of heavy and null water as a way to extract coordination information not only for the water-hydrogen (not possible from XRD due to the extremely weak hydrogen scattering) but also for the water-oxygen around the nitrate sites which has been only possible from XRD experiments. Moreover, this interplay provides rigorous ways (i) to identify the individual partial RDF's contributions to the total neutron-weighted distribution function (peak size and location), (ii) to isolate and assess the ion-pair formation, and (iii) to determine the actual nitrate–water coordination and corresponding hydrogen-bonding structure.^{65–67}

Therefore, the goal of this work is to explore the potential deconvolution of the contributions from water–nitrate correlations using neutron diffraction involving successive heavy- and null-aqueous solutions of KNO_3 under $^{14}\text{N}/^{15}\text{N}$ and $^{\text{nat}}\text{O}_{\text{N}}/^{18}\text{O}_{\text{N}}$ substitutions, *i.e.*, $\text{O}_w\cdots\text{O}_{\text{N}}$, $\text{H}\cdots\text{O}_{\text{N}}$, $\text{O}_w\cdots\text{N}$, and $\text{H}\cdots\text{N}$, to achieve a full characterization of the first water coordination around the nitrate ion. For that purpose, in section 2 we discuss the fundamentals underlying the first-order difference approach involving $^{14}\text{N}/^{15}\text{N}$ and $^{\text{nat}}\text{O}_{\text{N}}/^{18}\text{O}_{\text{N}}$ substitutions in aqueous KNO_3 solutions when the aqueous environments comprise either heavy or null water comple-

mented with a brief description of the Poirier–DeLap⁶⁸ approach to the determination of the degree of ion-pair association according to the extracted $\text{K}^+\cdots\text{NO}_3^-$ distribution function. In section 3 we describe the intermolecular potential models used in the simulation of the aqueous KNO_3 and the corresponding molecular dynamics simulation methodology, while in section 4 we discuss the microstructural behavior of the aqueous KNO_3 and its characterization of the coordinating water environments according to the proposed interplay. Finally, we close the work with a discussion and highlight of the most relevant findings to answer the question posed by the title.

2. FUNDAMENTALS

While the neutron diffraction involving water H/D and isotopic substitution on monatomic ionic species can be considered a mature approach for the microstructural studies of aqueous electrolyte solutions^{69–71} as long as we keep in mind the subtleties and difficulties behind the interpretation of NDIS raw data in the presence of ion-pairing,^{66,72,73} NDIS experiments on aqueous electrolytes involving $^{\text{nat}}\text{O}/^{18}\text{O}$ substitution are currently nonexistent obviously due to the short time elapsed since Fischer et al.'s findings.⁶² Considering the challenges underlying these experiments, it becomes extremely valuable to be able to have a “dry run” of these NDIS experiments by molecular simulation to determine the location of relevant diffraction peaks and the presence of peak overlapping and ultimately to aid the interpretation of the experimental evidence. For that reason, in the analysis that follows we illustrate what could be expected in a simulated NDIS experiment involving $^{\text{nat}}\text{O}/^{18}\text{O}$ and $^{14}\text{N}/^{15}\text{N}$ in aqueous nitrate solutions, where all microstructural details are known simultaneously with the corresponding first-order differences of the neutron-weighted distribution functions. This feature allows the unambiguous identification of peak overlappings between pair correlation functions and, consequently, the isolation of specific pair correlation peaks for the assessment of meaningful species coordination as well as the opportunity to test conjectured behaviors underlying the potential occurrence of ion-pairing and its effect in the interpretation of the NDIS raw data.^{66,67}

2.1. Neutron Diffraction with Isotopic Substitution and First-Order Difference Approach. The total structure factor $F(k)$ is the portion of the neutron scattering intensity from amorphous samples that can provide information on their microscopic structure,⁶⁹ *i.e.*,

$$F(k) = \sum_{i \leq j} (2 - \delta_{ij}) c_i c_j b_i b_j (S_{ij}(k) - 1) \quad (2.1)$$

where the magnitude of the scattering vector $k = (4\pi/\lambda) \sin(\theta/2)$ is expressed in terms of the wavelength λ of the incident neutrons and the scattering angle θ and c_i and b_i denote the atomic fraction and the coherent neutron scattering length of the atomic species i , respectively. Moreover, $S_{ij}(k)$ is the partial structure factor describing the correlation between atoms of types i and j , *i.e.*,

$$S_{ij}(k) = 1 + (4\pi\rho/k) \int_0^\infty [g_{ij}(r) - 1] r \sin(kr) dr \quad (2.2)$$

where ρ and $g_{ij}(r)$ are the atomic number density of the solution and the corresponding radial pair distribution function for ij -interactions. Note that the total structural factor $F(k)$ can

be extracted from either molecular simulation, usually in its real-space $G(r)$ counterpart (eq 2.3 as follows), or NDIS experiment.

For most practical purposes, such as the interpretation of experimental raw data, we would be dealing with the total (neutron-weighted real-space) pair correlation function $G(r)$ rather than $F(k)$, *i.e.*, its Fourier transform,

$$G(r) = \sum_{i \leq j} (2 - \delta_{ij}) c_i c_j b_i b_j (g_{ij}(r) - 1) \quad (2.3)$$

described as a linear combination of the corresponding radial pair distribution functions $g_{ij}(r)$, according to the following transformation,

$$g_{ij}(r) = 1 + (1/2\pi^2\rho_o r) \int_0^\infty [S_{ij}(k) - 1] k \sin(kr) dk \quad (2.4)$$

Because the structure of a simple $M^{+}X^{\nu-}$ aqueous solution (involving s scattering species) comprises $s(s+1)/2$ independent radial distribution functions $g_{ij}(r)$ (or partial structural factors $S_{ij}(k)$ for that matter), it would also require the same number of experiments (*i.e.*, involving different isotopic compositions) to extract the full set of $g_{ij}(r)$ (or $S_{ij}(k)$).⁷⁴ Moreover, the largest contribution to $G(r)$ comes from the (light, heavy, or their mixture) water–water correlation functions (either $g_{OH}(r)$ and $g_{HH}(r)$ or $g_{OD}(r)$ and $g_{DD}(r)$); consequently, the extraction of any relevant information about the local aqueous environment around the ions becomes challenging, if not impossible, under those conditions.

One way to circumvent this shortcoming is through the implementation of the *first-order difference* scheme⁷⁵ that comprises two diffraction experiments involving a pair of identical solutions except for the isotopic states of the ion (labeled α or β) under study. Under those conditions the first-order difference scheme allows the cancellation of contributions to $G(r)$ in eq 2.3 from the solvent–solvent and solvent–(nonsubstituted) solute species interactions; *i.e.*, for the case of nitrate ion we have that

$$\begin{aligned} \Delta G_N^{\text{solv}}(r) &= G_{^{14}\text{N}}^{\text{solv}}(r) - G_{^{15}\text{N}}^{\text{solv}}(r) \\ &= A_N(g_{O_wN}(r) - 1) + B_N(g_{DN}(r) - 1) \\ &\quad + C_N(g_{HN}(r) - 1) + D_N(g_{KN}(r) - 1) \\ &\quad + E_N(g_{NN}(r) - 1) + F_N(g_{O_NN}(r) - 1) \end{aligned} \quad (2.5)$$

for the nitrogen site (*i.e.*, $^{14}\text{N}/^{15}\text{N}$ substitution), or its normalized version,

$$\begin{aligned} \Delta G_N^{\text{solv},\text{norm}}(r) &= [A_N g_{O_wN}(r) + B_N g_{DN}(r) + C_N g_{HN}(r) + D_N g_{KN}(r) \\ &\quad + E_N g_{NN}(r) + F_N g_{O_NN}(r)] / \Sigma_N^{\text{solv}} \end{aligned} \quad (2.6)$$

Likewise,

$$\begin{aligned} \Delta G_O^{\text{solv}}(r) &= G_{^{16}\text{O}}^{\text{solv}}(r) - G_{^{18}\text{O}}^{\text{solv}}(r) \\ &= A_O(g_{O_wO_N}(r) - 1) + B_O(g_{DO_N}(r) - 1) \\ &\quad + C_O(g_{HO_N}(r) - 1) + D_O(g_{KO_N}(r) - 1) \\ &\quad + E_O(g_{O_NO_N}(r) - 1) + F_O(g_{NO_N}(r) - 1) \end{aligned} \quad (2.7)$$

for the nitrate's oxygen sites (*i.e.*, $^{16}\text{O}_N/^{18}\text{O}_N$ substitution), or its normalized form,

$$\begin{aligned} \Delta G_O^{\text{solv},\text{norm}}(r) &= [A_O g_{O_wO_N}(r) + B_O g_{DO_N}(r) + C_O g_{HO_N}(r) + D_O g_{KO_N}(r) \\ &\quad + E_O g_{O_NO_N}(r) + F_O g_{NO_N}(r)] / \Sigma_O^{\text{solv}} \end{aligned} \quad (2.8)$$

where the superscript solv describes the type of aqueous environment that in general could comprise light (lw), heavy (hw), or any mixture of both isotopic forms of water, whose special case becomes the null (nw) water (*vide infra*).

The prefactors of the six contributions in eqs 2.5–2.8 are given by $c_i c_j b_i [b_i^\alpha (2 - \delta_{ji}^\alpha) - b_i^\beta (2 - \delta_{ji}^\beta)]$, where we make explicit the isotopic dependence of the corresponding coherent neutron scattering lengths (b_i^l with $l = \alpha, \beta$) for the substituted species, and invoke Kronecker δ_{ji}^l for the corresponding pair of isotopic species, while the normalizing quantity in the denominator of eqs 2.6 and 2.8 is simply $\sum_l^{\text{solv}} A_l + B_l + C_l + D_l + E_l + F_l = -\Delta G_l^{\text{solv}}(0)$ for $l = \text{N, O}$.

Note that NDIS does not differentiate between oxygen species in H_2O and NO_3^- involving the same isotopic species, yet we made the distinction between O_w and O_N in the $\Delta G_N^{\text{solv}}(r)$ expressions to facilitate the interpretation of their contributions in the corresponding experimental raw data. In fact, this differentiation between O_w and O_N provides a tool to test the self-consistency of the experimental raw data sets, *i.e.*, $G_{\text{nat}(\text{NO}_3^-)}^{\text{solv}}(r)$, $G_{^{14}\text{N}}^{\text{solv}}(r)$, and $G_{^{15}\text{N}}^{\text{solv}}(r)$ by imposing the intramolecular coordination constraint $n_{\text{O}_N}^{\text{N}}(I_{\text{NO}}) = 3$ to both representations $\Delta G_N^{\text{solv}}(r) = G_{^{14}\text{N}}^{\text{solv}}(r) - G_{^{15}\text{N}}^{\text{solv}}(r)$, eq 2.5, and $\Delta G_O^{\text{solv}}(r) = G_{^{16}\text{O}}^{\text{solv}}(r) - G_{^{18}\text{O}}^{\text{solv}}(r)$, eq 2.7, respectively. With that purpose in mind we introduce the definition of intra-coordination and invoke eq 2.5, *i.e.*,

$$\begin{aligned} n_{\text{O}_N}^{\text{N}}(I_{\text{NO}}) &= 4\pi\rho_{\text{O}_N} \int_{I_{\text{NO}}-\delta}^{I_{\text{NO}}+\delta} g_{\text{NO}_N}(r) r^2 dr \\ &= (4\pi\rho_{\text{O}_N}/F_N) \int_{I_{\text{NO}}-\delta}^{I_{\text{NO}}+\delta} [\Delta G_N^{\text{solv}}(r) + \Sigma_N^{\text{solv}}] r^2 dr \end{aligned} \quad (2.9)$$

where $\Sigma_N^{\text{solv}} = A_N + B_N + C_N + D_N + E_N + F_N$. Likewise, from eq 2.7 we have that

$$\begin{aligned} n_{\text{O}_N}^{\text{O}}(I_{\text{NO}}) &= 4\pi\rho_{\text{O}} \int_{I_{\text{NO}}-\delta}^{I_{\text{NO}}+\delta} g_{\text{O}_N\text{N}}(r) r^2 dr \\ &= (4\pi\rho_{\text{O}}/F_O) \int_{I_{\text{NO}}-\delta}^{I_{\text{NO}}+\delta} [\Delta G_O^{\text{solv}}(r) + \Sigma_O^{\text{solv}}] r^2 dr \end{aligned} \quad (2.10)$$

with $\Sigma_O^{\text{solv}} = A_O + B_O + C_O + D_O + E_O + F_O$, where the parameter δ describes the spread of the distribution of the intramolecular bond length I_{NO} in the real system. Note that the equality of the

two lines in eqs 2.9 and 2.10 is guaranteed as long as there is no overlapping of peaks within the range of intramolecular interactions. From eqs 2.9 and 2.10 it becomes clear that the self-consistency of $\Delta G_N^{\text{solv}}(r)$ and $\Delta G_O^{\text{solv}}(r)$ means that

$$\begin{aligned} c_{O_N} F_N^{-1} \int_{l_{NO}-\delta}^{l_{NO}+\delta} [\Delta G_N^{\text{solv}}(r) + \Sigma_N^{\text{solv}}] r^2 dr \\ = c_N F_O^{-1} \int_{l_{NO}-\delta}^{l_{NO}+\delta} [\Delta G_O^{\text{solv}}(r) + \Sigma_O^{\text{solv}}] r^2 dr \end{aligned} \quad (2.11)$$

where the identity 2.11 becomes an indicator of properly normalized experimental first-order differences $\Delta G_O^{\text{solv, norm}}(r)$ and $\Delta G_N^{\text{solv, norm}}(r)$. Obviously, if the model system involves a rigid geometry for the nitrate ion, the bond-length distributions in eqs 2.9 and 2.10 become δ functions; *i.e.*, the constraint is satisfied by construction, and, consequently, $n_N^N(l_{NO}) = 4\pi \int \rho_{O_N N}(r) r^2 \delta(r - l_{NO}) dr = 3$.

Even though the water–water interactions cancel out in the first-order differences between two sets of $F(k)$ or $G(r)$ under isotopic substitutions, the choice of the isotopic form of the solvent water is crucial to alleviate the large source of uncertainties due to the unavoidably significant inelasticity (*i.e., aka* Placzek⁷⁶) corrections.⁷⁷ Of particular interest in the current study is the use of either heavy water or the (64% light–36% heavy) aqueous mixture,⁷⁸ *i.e.*, the so-called null-water (nw) solvent. In fact in Tables 3 and 4 we set $C_l = 0$ in eqs 2.5 and 2.6 for the heavy-water solutions, while $B_l = -C_l$ in eqs 2.7 and 2.8 for the null-water solutions since $c_D/c_H = -b_H/b_D \cong 0.5607$.⁶³ In particular, the use of a null-aqueous solution in combination with the more common heavy-aqueous counterpart is central to the proposed strategy to identify and isolate the diffraction peaks that define the aqueous coordination environment around the nitrate ion, while eliminating the spurious contributions of other overlapping peaks, as we will discuss and illustrate in section 4.

2.2. Ion-Pair Distribution Functions. The available experimental evidence from aqueous nitrate solutions involving a variety of cations provide evidence for the occurrence of either contact or water-shared ion-pairing.^{16,29,33,36,79–84} As previously discussed,^{65–67} ion-pair formation might have a significant effect on the interpretation of $\Delta G_l^{\text{nw, norm}}(r)$ ($l = N, O$) from NDIS experiments and the subsequent determination of coordination numbers. Given a set of microstructural data, it is possible to provide a meaningful and quantitative assessment of the ion-pair formation—through a precisely defined degree of ion-pair association—according to an unambiguous and rigorous formalism developed more than half a century ago by Poirier and DeLap⁶⁸ where we identify $\rightarrow NO_3^-$ and $+ \rightarrow K^+$, *i.e.*,

$$\alpha_{-+}(d_{-+}) = \int_0^{d_{-+}} G_{-+}(r) dr \quad (2.12)$$

where d_{-+} denotes the upper bound for the count of $NO_3^- \cdots K^+$ pairs and $G_{-+}(r)\Delta r$ gives the probability of finding the cation in the spherical shell of thickness Δr when the nearest anion locates at a distance r from the cation, while neither the cation nor the anion form any additional ion pair within the distance r . This formalism provides the link between the anion–cation radial distribution function $g_{-+}(r)$ and the ion-pair radial distribution function $G_{-+}(r)$ that for symmetric ion pairs reads as

$$G_{-+}(r) = 4\pi\rho_{-+}(r)r^2/[1 + 4\pi\rho_{-+} \int_0^r g_{-+}(s)s^2 ds]^2 \quad (2.13)$$

as described in detail in Appendix B.

3. POTENTIAL MODELS AND SIMULATION METHODOLOGY

In order to investigate the solvation behavior of the nitrate ion and to provide an illustration for the suggested method involving the dual isotopic substitution, *i.e.*, $^{14}\text{N}/^{15}\text{N}$ and $^{nat}\text{O}_N/^{18}\text{O}_N$, we performed isobaric–isothermal molecular dynamics simulations of a 3.5 m KNO_3 aqueous solution at ambient conditions according to the following intermolecular potential models. Water was described by the rigid SPC/E model,⁸⁵ the potassium cation according to Dang’s model,⁸⁶ and the nitrate anion by Krienke and Opalka’s⁵⁵ parametrization of the planar geometry (with $l_{NO} = 1.27 \text{ \AA}$ and $\angle O-N-O = 120^\circ$) based on the *ab initio* calculations of Lebrero et al.⁴⁶ as summarized in Table 1, *i.e.*,

$$\phi_{ij}(r_{ij}) = \sum_{\alpha \in i, \beta \in j} \{4\epsilon_{i_\alpha j_\beta} [(\sigma_{i_\alpha j_\beta}/r_{ij}^{\alpha\beta})^{12} - (\sigma_{i_\alpha j_\beta}/r_{ij}^{\alpha\beta})^6] + q_i^\alpha q_j^\beta / r_{ij}^{\alpha\beta}\} \quad (3.1)$$

Table 1. Potential Parameters for the Nitrate Ion,⁵⁵ Potassium Ion,⁸⁶ and SPC/E⁸⁵ Water Models

<i>ii</i> -interaction	$\epsilon_{ii}/k (K)^a$	$\sigma_{ii} (\text{\AA})^b$	$q_i(e)$
$O_N \cdots O_N$	78.07	3.154	-0.6201
$N \cdots N$	100.74	3.900	0.8603
$K \cdots K$	50.37	3.332	1.0
$O_W \cdots O_W$	78.23	3.166	-0.8476
$H \cdots H$			0.4238

$$^a \epsilon_{ij} = (\epsilon_{ii}\epsilon_{jj})^{1/2}, ^b \sigma_{ij} = 0.5(\sigma_{ii} + \sigma_{jj}).$$

with $r_{ij}^{\alpha\beta} = |\mathbf{r}_i^\alpha - \mathbf{r}_j^\beta|$ and \mathbf{r}_a^b denotes the vector position of site b on species a . Likewise, the ion–water interactions were represented by Lennard-Jones interactions between the water’s oxygen and either ion, plus the corresponding electrostatic interactions between all charged sites; *i.e.*,

$$\phi_{wi}(r_{iw}) = \sum_{\alpha \in i} 4\epsilon_{Oi_\alpha} [(\sigma_{Oi_\alpha}/r_{Oi}^\alpha)^{12} - (\sigma_{Oi_\alpha}/r_{Oi}^\alpha)^6] + \sum_{\alpha \in i, \beta \in w} q_i^\alpha q_w^\beta / r_{iw}^{\alpha\beta} \quad (3.2)$$

with $r_{Oi}^\alpha = |\mathbf{r}_O - \mathbf{r}_i^\alpha|$, $r_{iw}^{\alpha\beta} = |\mathbf{r}_i^\alpha - \mathbf{r}_w^\beta|$, and w identifies water sites, where the Lennard-Jones potential parameters for the unlike-pair interactions in eqs 3.1 and 3.2 are described by the Lorentz–Berthelot combining rules.

From the 10 simulated RDFs we determined the first-order differences of neutron-weighted radial distribution functions, for the heavy water— $\Delta G_N^{\text{hw}}(r) = G_{^{18}\text{O}_N}^{\text{hw}}(r) - G_{^{15}\text{N}}^{\text{hw}}(r)$ and $\Delta G_O^{\text{hw}}(r) = G_{^{18}\text{O}}^{\text{hw}}(r) - G_{^{nat}\text{O}}^{\text{hw}}(r)$ —and the null water— $\Delta G_N^{\text{nw}}(r) = G_{^{18}\text{O}_N}^{\text{nw}}(r) - G_{^{15}\text{N}}^{\text{nw}}(r)$ and $\Delta G_O^{\text{nw}}(r) = G_{^{18}\text{O}}^{\text{nw}}(r) - G_{^{nat}\text{O}}^{\text{nw}}(r)$ —for the two isotopic substitutions in NO_3^- , which will be later used for the estimation of the corresponding coordination numbers as well as the analysis of ion-pair formation.

The isobaric–isothermal molecular dynamics simulations of the aqueous solutions involved $N = 2048$ particles (*i.e.*, 1818 water molecules and 230 ions) and were carried out according to our own implementation of a Nosé–Poincare algorithm^{87,88} for the integration of the Newton–Euler equations of motion within a cubic simulation box under three-dimensional (3D) periodic boundary conditions. The initial configurations were

either taken from an *fcc* structure with randomly distributed species type or generated by the *Packmol* utility⁸⁹ and equilibrated by at least 1.0 ns, followed by production runs of 4.0 ns, using an integration time step of 2.0 fs. All Lennard-Jones interactions were truncated at a cutoff radius $r_c \approx 3.5\sigma_{\text{SPCE}}$ where the configurational energy and virial were corrected *on the fly* by the corresponding long-range contributions, while the electrostatic interactions were handled by an Ewald summation whose convergence parameters were chosen to ensure an error smaller than $5 \times 10^{-5}\epsilon_{\text{SPCE}}$ for both the real and reciprocal spaces.⁹⁰

4. MICROSTRUCTURAL RESULTS

In what follows we analyze the simulated behavior of the neutron-weighted pair correlation functions for the $^{14}\text{N}/^{15}\text{N}$ and $^{\text{nat}}\text{O}_\text{N}/^{18}\text{O}_\text{N}$ substitutions in the nitrate ion in heavy- and null-water environments. In Table 2 we collect the values of the coherent scattering lengths used in the study, which were taken from the available literature.

Table 2. Coherent Neutron Scattering Lengths Used in This Study

species	$b_{\text{coh}}(\text{fm})$	ref
^{14}N	9.37	63
^{15}N	6.44	63
$^{\text{nat}}\text{N}$	9.36	63
^2H	6.67	63
$^{\text{nat}}\text{O}$	5.805	63
^{18}O	6.009	62
$^{\text{nat}}\text{K}$	3.67	63

For interpretational purposes we determine the individual contributions from each pair interaction to the corresponding first-order difference $\Delta G_N^{\text{solv},\text{norm}}(r)$ and $\Delta G_O^{\text{solv},\text{norm}}(r)$, *i.e.*, eqs 2.6 and 2.8 for both types of solvents. In Tables 3 and 4 we

Table 3. Coefficients of the First-Order Difference of Weighted Distributions for the $^{14}\text{N}/^{15}\text{N}$ Substitution in Heavy and Null Water

coefficient ^a	heavy water	null water
A_N	0.1956595	0.1956595
B_N	0.4496293	0.1614901
C_N	0.0	-0.1614901
D_N	7.824720×10^{-3}	7.824720×10^{-3}
E_N	1.685406×10^{-2}	1.685406×10^{-2}
F_N	3.713011×10^{-2}	3.713011×10^{-2}
\sum_N^{solv}	0.7070977	0.2574684

^aIn fm² units.

display the coefficients of the two sets of first-order differences, where we can observe the contrasting magnitudes of these coefficients not only for the pair interactions, *i.e.*, $A_l, B_l > D_l, E_l, F_l$, but also for the type of isotopic substitution, *i.e.*, $A_N, B_N \gg A_O, B_O$. Obviously, the first inequality indicates that the two more significant contributions to $\Delta G_l^{\text{solv},\text{norm}}(r)$ come from the pair interactions between the *l*-substituted species and the surrounding water, while the second inequality is simply a manifestation of the smaller change of coherent scattering length for the $^{\text{nat}}\text{O}_\text{N}/^{18}\text{O}_\text{N}$ in comparison with the $^{14}\text{N}/^{15}\text{N}$ substitution (see also Table 2).

Table 4. Coefficients of the First-Order Difference of Weighted Distributions for the $^{\text{nat}}\text{O}_\text{N}/^{18}\text{O}_\text{N}$ Substitution in Heavy and Null Water

coefficient ^a	heavy water	null water
A_O	4.086813×10^{-2}	4.086813×10^{-2}
B_O	9.391575×10^{-2}	3.375904×10^{-2}
C_O	0.0	-3.375904×10^{-2}
D_O	1.634378×10^{-3}	1.634378×10^{-3}
E_O	7.755504×10^{-3}	7.755504×10^{-3}
F_O	7.891768×10^{-3}	7.891768×10^{-3}
\sum_O^{solv}	0.1520655	5.814978×10^{-2}

^aIn fm² units.

In Figures 1 and 2 we display the partial contributions from the relevant individual pair interactions and the resulting

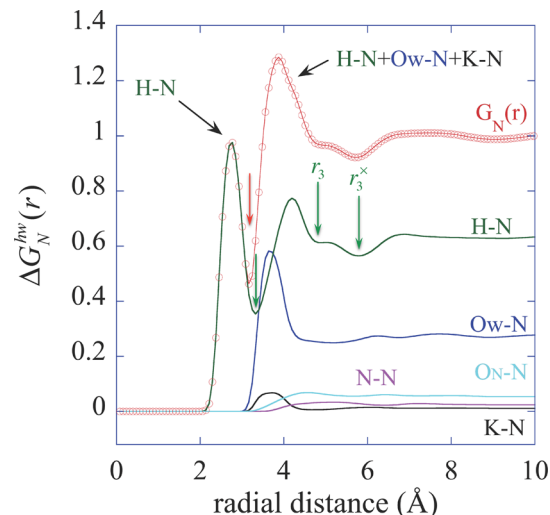


Figure 1. Partial contributions of the five relevant pair correlation functions to the normalized *neutron-weighted distribution functions* $\Delta G_N^{\text{hw}}(r)$ of a 3.5 M heavy-aqueous KNO_3 solution at ambient conditions. The red and green arrows highlight the locations of the upper radial distance of integration r_u in the equations of footnotes ^a and ^b of Table 5, and the corresponding r_3 and r_3^* in the equations of footnotes ^a and ^b in Table 6.

neutron-weighted pair correlation functions $\Delta G_N^{\text{hw},\text{norm}}(r)$ and $\Delta G_O^{\text{hw},\text{norm}}(r)$, respectively. The main features in $\Delta G_N^{\text{hw},\text{norm}}(r)$ are the location of the two prominent peaks at 2.77 and 3.87 Å corresponding to the nearest D···N interactions, and the combination of contributions from the second nearest D···N, the $\text{O}_\text{w}^\text{..N}$, and the contact K···N pair interactions. Due to the overlapping of $\text{O}_\text{w}^\text{..N}$, K···N, and D···N correlation peaks within $3.2 \leq r (\text{\AA}) \leq 4.7$, neither can we take the location of the second peak of $\Delta G_N^{\text{hw},\text{norm}}(r)$ as that for the second D···N coordination nor estimate the coordination by integration of that peak.

Moreover, according to Figure 1, the first peak of $\Delta G_N^{\text{hw},\text{norm}}(r)$ comprises most but not all contribution from the first peak of the corresponding $g_{\text{DN}}(r)$. Consequently, the eventual calculation of the first coordination number $n_D^N(r)$ by integration of $\Delta G_N^{\text{hw},\text{norm}}(r)$ as usually done,²⁰ *i.e.*,

$$n_D^N(r) = (4\pi\rho_D \sum_N^{\text{hw}} / B_N^{\text{hw}}) \int_{r_1}^{r_2} \Delta G_N^{\text{hw},\text{norm}}(r) r^2 dr \quad (4.1)$$

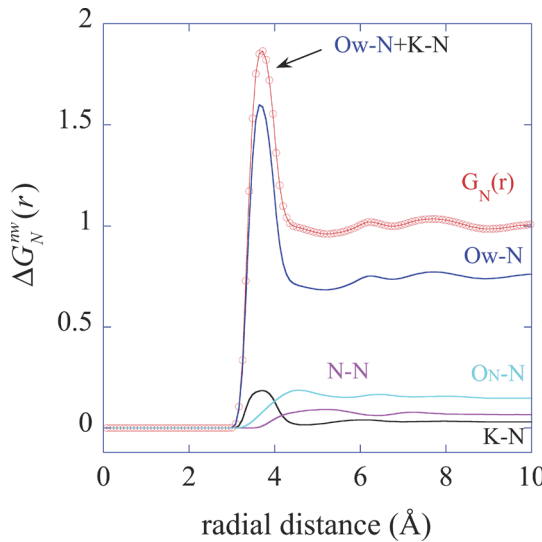


Figure 2. Partial contributions of the five relevant pair correlation functions to the normalized neutron-weighted distribution functions $\Delta G_N^{nw}(r)$ of a 3.5 m null-aqueous KNO_3 solution at ambient conditions.

would result in an underestimation of the coordination number because the upper limit of integration $r_2 \approx 3.16 \text{ \AA}$, corresponding to the location of the first minimum of $\Delta G_N^{hw,\text{norm}}(r)$, is slightly smaller than the actual value of $r_u \approx 3.32 \text{ \AA}$ from the $g_{DN}(r)$ (see arrows in Figure 1). In fact, the direct determination of $n_D^N(r)$ using eq A3 indicates that the (true) first coordination number $n_D^N(r_u \approx 3.32 \text{ \AA}) \cong 5.9$ while the estimated value from eq 4.1 is $n_D^N(r_u \approx 3.17 \text{ \AA}) \cong 5.2$ which is in rather good agreement with $n_D^N(r_u \approx 3.15 \text{ \AA}) \cong 5.0 \pm 0.5$ as reported by Kameda et al.²⁰ based on the same equation. This comparison highlights a frequently hidden fact; *i.e.*, the equivalence between the true coordination given by eq A3 and the NDIS-related coordination relies on the absence of any contribution from other correlations in the $[r_1, r_2]$ radial interval. Moreover, should other correlations be contributing, then the actual values for r_1 and r_2 might not be precisely the same in eq A3 and eq 4.1 as is clearly obvious by the parenthetical values in Table 5 and corresponding arrows in Figure 1.

Table 5. First Water Coordination of the Nitrate Ion According to the Direct and the NDIS-Based Expressions

$\alpha\cdots\beta$ -interactions	direct integral (r_u) ^a	NDIS integral (r_u) ^b
$\text{O}_w\cdots\text{N}$	14.5 (5.15 \AA)	19.9 (5.22 \AA) ^c
$\text{D}\cdots\text{N}$	5.9 (3.32 \AA)	5.2 (3.17 \AA) ^d
$\text{O}_w\cdots\text{O}_N$	2.1 (3.24 \AA)	2.4 (3.24 \AA) ^c
$\text{D}\cdots\text{O}_N$	2.0 (2.53 \AA)	1.9 (2.54 \AA) ^d
$\text{K}\cdots\text{N}$	1.3 (5.8 \AA)	

^a $n_\alpha^\beta(r_u) = 4\pi\rho_\alpha \int_0^{r_u} g_{\alpha\beta}(r)r^2 dr$. ^b $n_\alpha^\beta(r_u) = (4\pi\rho_\alpha \sum_\beta I_{\alpha\beta}^{\text{solv}}) \int_0^{r_u} \Delta G_{\beta\text{solv},\text{norm}}(r)r^2 dr$; with solv = (hw,nw) and $I_{\alpha\beta}^{\text{solv}} = (A_{\alpha\beta}^{\text{solv}} \text{ if } \alpha = \text{O}_w \text{ or } B_{\beta}^{\text{solv}} \text{ if } \alpha = \text{D})$. ^c Null water. ^d Heavy water.

If we now switch to the null-aqueous environment, Figure 2, we observe the absence of contributions to $\Delta G_N^{nw,\text{norm}}(r)$ from hydrogen interactions where the main peak, centered at $r \approx 3.66 \text{ \AA}$, comprises two main contributions, *i.e.*, the major from $\text{O}_w\cdots\text{N}$ interactions that overlap with the contact $\text{K}\cdots\text{N}$ pair configurations. There are, however, two smaller contributions

from the shoulders of the $\text{N}\cdots\text{N}$ and the $\text{O}_N\cdots\text{N}$ pair correlation peaks that might affect the outcome of the conventional determination of the water coordination around the nitrogen site, *i.e.*,

$$n_{\text{O}_w}^N(r_u) = (4\pi\rho_{\text{O}_w} \Sigma_N^{\text{nw}} / A_N^{\text{nw}}) \int_0^{r_u} \Delta G_N^{\text{nw},\text{norm}}(r)r^2 dr \quad (4.2)$$

In Table 5 we collect the resulting water-oxygen coordination around the nitrogen site of the nitrate ion, according to the direct integration of the $g_{\text{O}_w\text{N}}(r)$, the integral of footnote ^a of Table 5, and the NDIS-based estimate based on eq 4.2. From this comparison we find, not surprisingly, that the latter overestimates the coordination due to the contributions from the overlapping correlations. Note that earlier XRD experiments on aqueous $\text{Zn}(\text{NO}_3)_2$ by Dagnall et al.⁵ resulted in a $n_{\text{O}_w}^N(r_u) \approx 17.7 \pm 2.8$.

In Figures 3 and 4 we display the corresponding $\Delta G_O^{hw,\text{norm}}(r)$ and $\Delta G_O^{\text{nw},\text{norm}}(r)$ counterparts to Figures 1 and 2. Note that

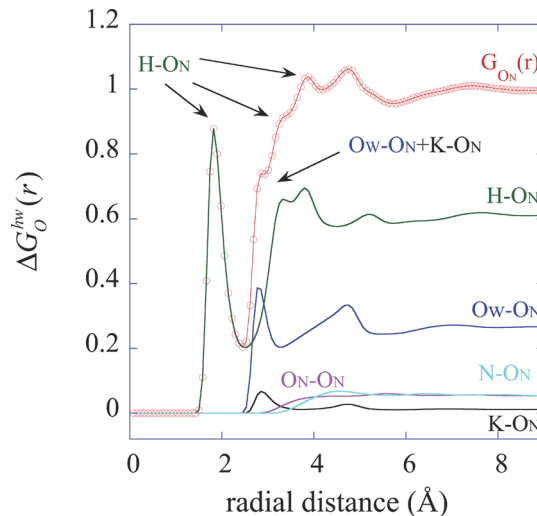


Figure 3. Partial contributions of the five relevant pair correlation functions to the normalized neutron-weighted distribution functions $\Delta G_O^{hw}(r)$ of a 3.5 m heavy-aqueous KNO_3 solution at ambient conditions.

$\Delta G_O^{hw,\text{norm}}(r)$ exhibits a fully decoupled first peak associated with the $\text{D}\cdots\text{O}_N$ correlations centered at $r \approx 1.8 \text{ \AA}$ resembling the corresponding $\text{D}\cdots\text{O}_w$ peak for pure water,⁹¹ followed by a bumpy and wider peak that result from the overlapping among the second $\text{D}\cdots\text{O}_N$ coordination, the $\text{K}\cdots\text{O}_N$, and the $\text{O}_w\cdots\text{O}_N$ correlations.

While the decoupling of the first peak in Figure 3 suggests that its integral will provide an accurate estimate—by comparison against the corresponding integral of footnote ^a of Table 5—for the first coordination of water-hydrogen around the nitrate-oxygens as clearly depicted in Table 5, there are no chances for a decoupling toward an estimation of the second water-hydrogen coordination. In contrast, the first peak of $\Delta G_O^{\text{nw},\text{norm}}(r)$ in Figure 4 comprises mostly contribution from $\text{O}_w\cdots\text{O}_N$ interactions centered at $r \approx 2.8 \text{ \AA}$, bearing similarities to that for $\text{O}_w\cdots\text{O}_w$ in pure water,⁹¹ while overlapping a smaller contribution from the contact $\text{K}\cdots\text{O}_N$ pair configurations. This behavior precludes an accurate calculation of the water-oxygen coordination around the nitrate-oxygen by

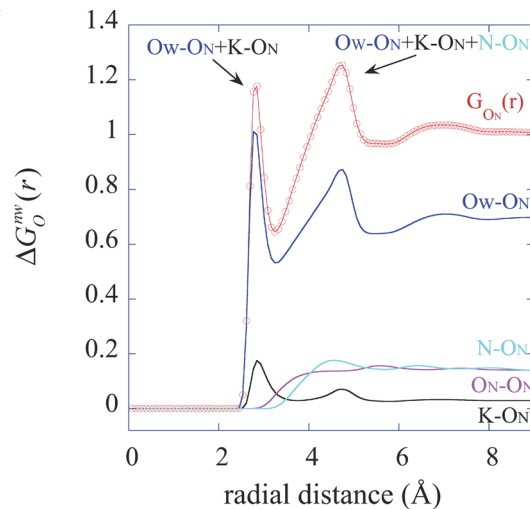


Figure 4. Partial contributions of the five relevant pair correlation functions to the normalized neutron-weighted distribution functions $\Delta G_O^{nw}(r)$ of a 3.5 m null-aqueous KNO_3 solution at ambient conditions.

$$n_{O_w}^{ON}(r_u) = (4\pi\rho_{O_w}\Sigma_{O_w}^{nw}/A_O^{nw}) \int_0^{r_u} \Delta G_O^{nw,\text{norm}}(r)r^2 dr \quad (4.3)$$

in comparison to the direct integral over $g_{O_wON}(r)$, where in the present case, the NDIS-related method slightly overestimates $n_{O_w}^{ON}(r_u)$ as illustrated in Table 5.

Obviously, the degree of discrepancy between these two outcomes depends mainly on the extent of $\text{K}\cdots\text{O}_N$ pair formation, *i.e.*, the size of the contribution due to the overlapping between $\text{K}\cdots\text{O}_N$ and $O_w\cdots\text{O}_N$ peaks as clearly highlighted by Figure 4. Moreover, note that the second peak of $\Delta G_O^{nw,\text{norm}}(r)$ centered at $r \approx 4.7 \text{ \AA}$, resulting from the overlapping contribution of the solvent-shared $\text{K}\cdots\text{O}_N$ pair and $\text{N}\cdots\text{O}_N$ interactions, suggests that the water-oxygen sites and the nitrate-oxygen-site counterparts are located at the corners of a deformed tetrahedral configuration.

While the idea of a tetrahedral distribution between the nitrate-oxygens and water-oxygens, where each nitrate-oxygen coordinates three water-oxygens, was suggested by Caminiti et al.⁴ (see their Figure 3) and Dagnall et al.⁸ However, according to Table 5, the current molecular models describe bicoordination rather than tricoordination suggested by these authors. Moreover, and contrary to the frequently used assumption in the interpretation of XRD data,^{5,92,93} Table 5 also highlights the fact that the water coordination of nitrate-nitrogen should not necessarily be taken to be three times that of the corresponding nitrate-oxygens, *i.e.*, $n_{O_w}^{ON}(r_u) \neq 3n_{O_w}^{ON}(r_u)$. The failure of such a conjecture hinges around the fact that the radii of the coordination shells for these two types of interactions are significantly different (see Table 5).

A recurrent issue regarding nitrate hydration is the weakness of the water-anion interactions whose immediate outcome has been the assumption about the absence of a second water coordination around the nitrate ion in the modeling of XRD experiments,⁹⁴ whose clear representative would be a second nearest $\text{D}\cdots\text{N}$ correlation peak centered at $r \sim 4.1 \text{ \AA}$ as conjectured by Kameda et al.²⁰ In fact, our simulations describe the $g_{DN}(r)$ exhibiting two prominent peaks centered at $r \sim 2.7 \text{ \AA}$ and $r \sim 4.1 \text{ \AA}$, respectively, as clearly depicted by the green

line in Figure 1. Obviously, the heavy-water-based NDIS experiment alone will not be able to identify (or deconvolute) explicitly such a peak (*e.g.*, see Figure 4 of ref 20), but, according to Figures 1 and 2, we can in principle extract this alleged second coordination number $n_D^N(r_2, r_3)$ by applying the following difference (see Appendix A for details),

$$n_D^N(r_2, r_3) = (4\pi\rho_D/B_N^{hw}) \int_{r_2}^{r_3} [\Sigma_N^{hw} \Delta G_N^{hw,\text{norm}}(r) - \Sigma_N^{nw} \Delta G_N^{nw,\text{norm}}(r)] r^2 dr \quad (A4)$$

where r_2 and r_3 denote the location of the minima defining the second peak of the $g_{DN}(r)$. In Table 6 we display the

Table 6. Second Water-Hydrogen Coordination of the Nitrate Ion According to the Direct and the Derived NDIS-Based Expressions

$\alpha\cdots\beta$ -interactions	direct integral (r_2, r_3 or r_3^\times) ^a	NDIS integral (r_2, r_3 or r_3^\times) ^b
D \cdots N	18.2 (3.32 Å, 4.83 Å)	18.8 (3.17 Å, 4.83 Å)
D \cdots N	36.1 (3.32 Å, 5.77 Å)	36.8 (3.17 Å, 5.77 Å)
$a n_D^N(r_u) = 4\pi\rho_D \int_{r_2}^{r_3} g_{DN}(r) r^2 dr$	$b n_D^N(r) = (4\pi\rho_D/B_N^{hw}) \int_{r_2}^{r_3} [\Sigma_N^{hw} \Delta G_N^{hw,\text{norm}}(r) - \Sigma_N^{nw} \Delta G_N^{nw,\text{norm}}(r)] r^2 dr$	

comparison between the second coordination numbers resulting from the direct integration of $g_{DN}(r)$ and the proposed NDIS approach, where we chose two alternative upper values, r_3 or r_3^\times , for the integral as highlighted in Figure 1.

A relevant microstructural feature in Figures 1–4 is linked to the occurrence of $\text{NO}_3^- \cdots \text{K}^+$ pair association defined in terms of the radial pair distribution function $g_{KN}(r)$ whose corresponding ion-pair distribution functions $G_{-+}(r)$ and the resulting degree of ion-pair association $\alpha_{-+}(r)$ (discussed in section 2.2) are plotted in Figure 5. Note the relatively strong first peak for the $g_{KN}(r)$ representing the contact ion-pair conformation centered at $r \sim 3.7 \text{ \AA}$ and followed by weaker water-shared ion-pair configuration centered at $r \sim 6.1 \text{ \AA}$. The corresponding $G_{-+}(r)$ function exhibits a behavior that resembles that of $g_{KN}(r)$, though slightly shifted to the left and with a much smaller magnitude resulting from the

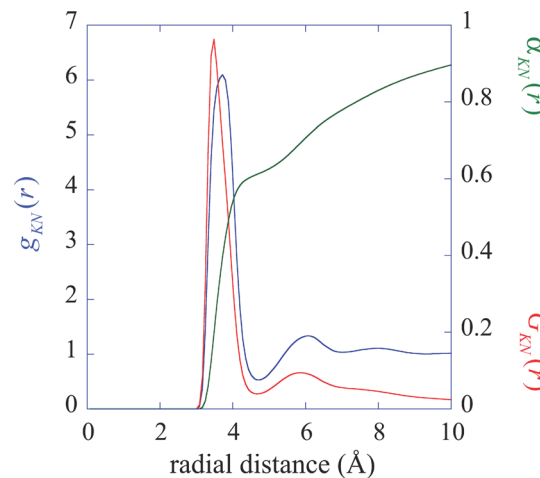


Figure 5. Radial pair distribution function $g_{KN}(r)$, the corresponding Pourier-DeLap $\text{K}^+ \cdots \text{NO}_3^-$ pair distribution function, and the resulting degree of pair association for a 3.5 m aqueous KNO_3 solution at ambient conditions.

normalization of its integral to one. Moreover, we also display the radial integral of $G_{-+}(r)$ that measures the degree of $\text{NO}_3^- \cdots \text{K}^+$ pair association, in this case $\alpha(\text{CIP}) \cong 0.6$ and $\alpha(\text{CIP+SShIP}) \cong 0.78$ for the simulated 3.5 m aqueous KNO_3 environments.

5. DISCUSSION AND FINAL REMARKS

Despite the relevance and ubiquitous nature of the nitrate ion we currently suffer from a rather deficient knowledge of its aqueous coordination behavior. On the one hand, the prolific XRD activities have not been able to produce a consistent picture due to the weak hydrogen scattering and the consequent involvement of conjectures regarding the relative location of the water-hydrogens. On the other hand, the conventional heavy-water NDIS of the nitrogen species “buries” the contribution from the hydration of the nitrate-oxygens under the contributions of the second water-hydrogen shell around the nitrate-nitrogen. In order to circumvent both limitations, and to attempt a novel strategy, we have developed a simulation analysis to test the *theoretical feasibility* of performing NDIS experiments involving heavy- and null-aqueous solutions of KNO_3 under $^{14}\text{N}/^{15}\text{N}$ and $^{\text{nat}}\text{O}_\text{N}/^{18}\text{O}_\text{N}$ substitutions aimed at achieving a full characterization of the first water coordination around the nitrate ion.

Due to the challenging nature of any NDIS, especially those involving null-aqueous environments, our molecular simulation analysis allows taking an atomistic “peek” at the local environment around the two labeled nitrate sites prior to any experimental attempt. Moreover, because the underlying molecular simulation provides the 10 RDFs defining the system microstructure, we are able to “reconstruct” the NDIS output from the relevant distribution functions and, consequently, test the accuracy of the “measured” NDIS-based coordination numbers (footnote ^b in Table 5) against the “direct” counting (footnote ^a in Table 5) from the simulated microstructure. In this context, theoretical feasibility means that the proposed tool provides us the means (a) to identify the individual partial RDF’s contributions to the total neutron-weighted distribution function (peak size and radial location), (b) to isolate the ion-pair configurations and assess their contribution to the NDIS raw data, (c) to “dig up” the hydration behavior of the nitrate-oxygens, and consequently be able (d) to determine the actual water coordination around the nitrogen and oxygen sites of the nitrate ion.

To provide a deeper understanding of the nitrate coordination we analyze the microstructural behavior of water around the ion in terms of the spatial distribution functions for the $\text{N} \cdots \text{X}_w$ interactions, $g_{\text{NX}_w}(r, \theta, \phi)$.⁹⁵ For that purpose, in what follows, the polar angle θ is defined between the principal z -axis (direction perpendicular to the plane defining the nitrate geometry) and the vector position r (relative to the molecule at the origin of the principal axes) of the neighboring water molecule, while the azimuthal angle ϕ is the angle formed between the principal y -axis and the projection of r onto the $z = 0$ plane as depicted in Figure 6.

According to the principal axes of Figure 6, we define the following distribution functions,

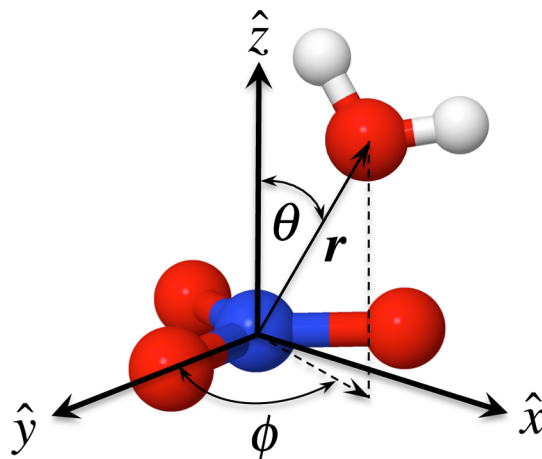


Figure 6. Principal axes centered at the nitrogen site of the nitrate model whose rigid geometry lies in the $\hat{x}-\hat{y}$ plane where one of the $\text{N}-\text{O}$ bonds locates along the \hat{y} axis.

$$\begin{aligned} g_{\text{NX}_w}(r, \theta, \phi) \\ = \frac{V \langle \sum_i \sum_{j \neq i} n_{\text{NX}_w}(r_{ij} \pm 0.5\delta_r, \theta_{ij} \pm 0.5\delta_\theta, \phi_{ij} \pm 0.5\delta_\phi) \rangle}{\delta V(r_{ij} \pm 0.5\delta_r, \theta_{ij} \pm 0.5\delta_\theta, \phi_{ij} \pm 0.5\delta_\phi) N_N N_{X_w}} \end{aligned} \quad (5.1)$$

where $n_{\text{NX}_w}(\dots)$ denotes a conditional number of $\text{N} \cdots \text{X}_w$ interactions and N_N and N_{X_w} are the total numbers of nitrate ions and X sites of the water molecules, respectively, while the explicit form of the volume element in the denominator of eq 5.1 becomes⁹⁶

$$\begin{aligned} \delta V &= \int_{r-0.5\delta_r}^{r+0.5\delta_r} r^2 dr \int_{\theta-0.5\delta_\theta}^{\theta+0.5\delta_\theta} \sin \theta d\theta \int_{\phi-0.5\delta_\phi}^{\phi+0.5\delta_\phi} d\phi \\ &= 2(r^2 \delta_r + \delta_r^3 / 12) \sin \theta \sin(0.5\delta_\theta) \delta_\phi \end{aligned} \quad (5.2)$$

where we have used $\delta_r = 0.08 \text{ \AA}$ and $\delta_\theta = \delta_\phi = 5^\circ$ in all of the simulations. Note that the radial distribution functions used in the previous sections are simply the orientationally averaged $g_{\text{NX}_w}(r) \equiv \langle g_{\text{NX}_w}(r, \theta, \phi) \rangle_{\theta, \phi}$ counterparts of those given by eq 5.1, as illustrated in Figure 7, and portray a weak mean interaction of water with the nitrate’s nitrogen core represented by a single $\text{N} \cdots \text{O}_w$ peak at $r \sim 3.6 \text{ \AA}$ (p_1) and sandwiched between the double $\text{N} \cdots \text{H}_w$ peaks located at $r \sim 2.7 \text{ \AA}$ (p_1) and $r \sim 4.2 \text{ \AA}$ (p_2), respectively. However, the actual spatial (*i.e.*, orientationally dependent) distribution of the $\text{N} \cdots \text{X}_w$ pair interactions exhibits a preference for specific orientations that translates into stronger correlations several times larger than the corresponding angle-averaged quantities shown in Figure 7. To make this explicit, we display the behavior of the spatial distribution function $g_{\text{NX}_w}(r, \theta)_{\phi=\text{const}}$ for $X_w = \{\text{H}_w, \text{O}_w\}$ at three representative values of the azimuthal angle, namely, $\phi = 0^\circ$, $\phi = 60^\circ$, and $\phi = 90^\circ$. These three azimuthal angles were chosen as reference orientations since $\phi = 0^\circ$ represents the distributions in the plane perpendicular to the nitrate’s rigid geometry containing the bond; $\phi = 60^\circ$ defines the distribution on the plane bisecting the $\angle \text{O}_1-\text{N}-\text{O}_2$ angle and containing the $\text{N}-\text{O}_3$ bond (see Figure 6), *i.e.*, it describes a plane of symmetry; and $\phi = 90^\circ$ characterizes the distribution on the

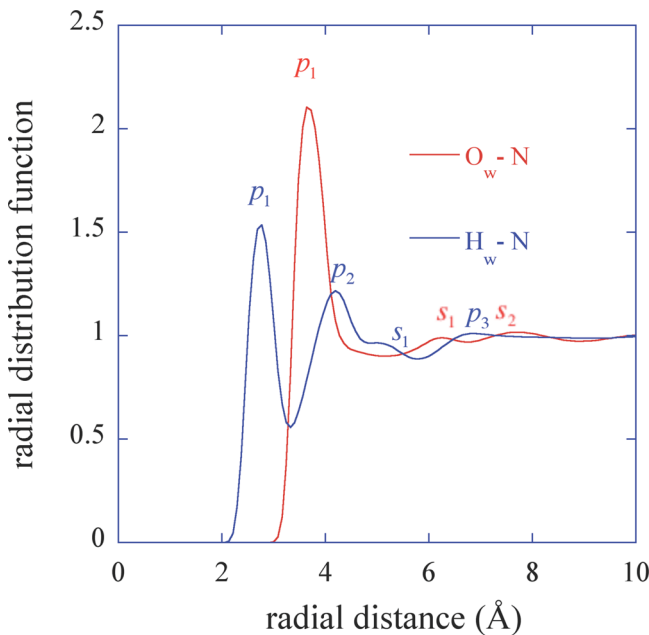


Figure 7. Radial pair distribution functions $g_{XwN}(r)$ for the nitrate-nitrogen/water-site interactions in the 3.5 m aqueous KNO_3 solution at ambient conditions. The notation s_j and p_j denote the j th shoulder and peak of interest, respectively.

plane containing the N site and perpendicular to the $\text{N}-\text{O}_1$ bond.

In Figure 8a–c we illustrate how the three correlation peaks in $g_{\text{NH}_w}(r,\theta)_{\phi=0^\circ}$ evolve as we increase the azimuthal angle from $\phi = 0^\circ$ to $\phi = 90^\circ$, where the major changes occur at the nearest water-hydrogen neighbors, *i.e.*, p_1 peaks. The strong double p_1 peak for $\phi = 0^\circ$, centered at $\theta \sim 40^\circ$ and $\theta \sim 140^\circ$, transitions first to a single peak centered at $\theta \sim 60^\circ$ as $\phi \rightarrow 60^\circ$ and then widens and increases its strength as $\phi \rightarrow 90^\circ$. Interestingly, in the same process the $\{p_j, s_j\}$ peaks exhibit negligible changes in strength or location within the $0 \leq \phi$ (deg) ≤ 90 range. In contrast, and due to water's H_w/O_w site ratio, $g_{\text{NO}_w}(r,\theta)_{\phi=\text{const}}$ in Figure 9a–c comprises fewer correlation peaks than $g_{\text{NH}_w}(r,\theta)_{\phi=\text{const}}$ (Figure 8a–c), although its behavior with increasing azimuthal angle follows the same trend as the latter. Therefore, the spatial distribution functions $g_{\text{N}X_w}(r,\theta,\phi)$ offer a detailed picture about the inhomogeneous water local environment around the nitrate ion within the hydration shell of radius $r < 7 \text{ \AA}$, while $g_{\text{N}X_w}(r>7\text{\AA},\theta,\phi) \approx 1.0$. This behavior could not have been anticipated from the sole analysis of the corresponding $g_{\text{N}X_w}(r)$.

At this point we conclude the discussion with the answer to the question posed by the title of this work which can be summarized as follows. On the one hand, our study of the aqueous solutions of KNO_3 under $^{14}\text{N}/^{15}\text{N}$ substitution suggests that (1) the null-water NDIS-based water-oxygen coordination around the nitrogen site of the nitrate ion, $n_{\text{O}_w}^{\text{N}}(r_u)$, tends to overestimate the actual coordination because the corresponding first-order difference contains (overlapped) contributions mainly from $\text{K}\cdots\text{N}$ contact pair configurations, and (2) the heavy-water NDIS-based water-hydrogen coordination around the nitrogen site of the nitrate ion, $n_{\text{D}}^{\text{N}}(r_u)$, exhibits a propensity to underestimate the true coordination because the partial overlapping of the first peaks of the $\text{D}\cdots\text{N}$

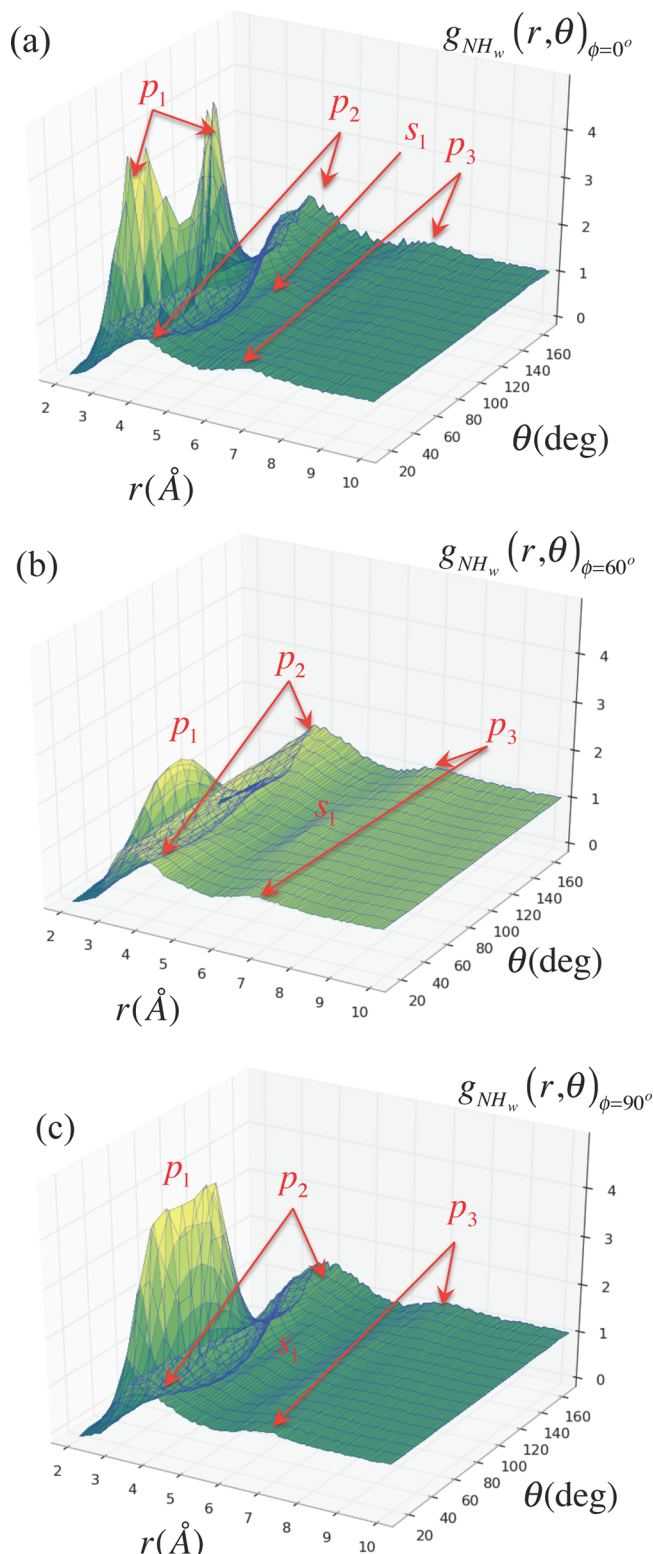


Figure 8. Spatial pair distribution functions $g_{\text{NH}_w}(r,\theta)_{\phi=\text{const}}$ for the 3.5 m aqueous KNO_3 solution at ambient conditions: (a) at $\phi = 0^\circ$, (b) at $\phi = 60^\circ$, and (c) at $\phi = 90^\circ$ where (s_j, p_j) denotes the j th shoulder or peak of the $g_{\text{NH}_w}(r)$ in Figure 7.

and the $\text{O}_w\cdots\text{N}$ pair correlations. On the other hand, our study of the aqueous solutions of KNO_3 under $^{nat}\text{O}_N/^{18}\text{O}_N$ substitution suggests that (3) the null-water NDIS-based water-oxygen coordination around the oxygen site of the

Figure 9-a

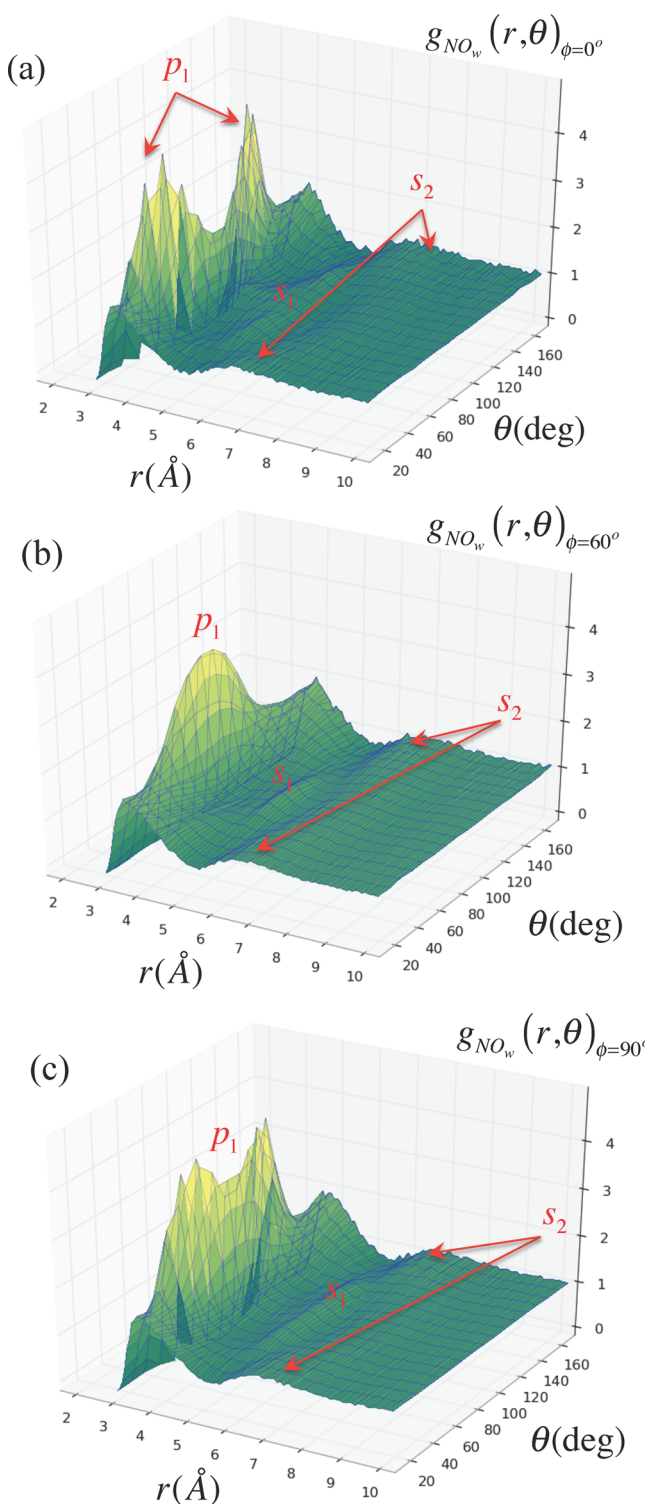


Figure 9. Spatial pair distribution functions $g_{NO_w}(r, \theta)_{\phi=\text{const}}$ for the 3.5 m aqueous KNO_3 solution at ambient conditions: (a) at $\phi = 0^\circ$, (b) at $\phi = 60^\circ$, and (c) at $\phi = 90^\circ$, where (s_j, p_j) denotes the j th shoulder or peak of the $g_{NO_w}(r)$ in Figure 7.

nitrate ion, $n_{\text{O}_w}^{\text{O}_N}(r_u)$, tends to overestimate the actual coordination because of the partial overlapping between the first peaks of the $\text{O}_w\cdots\text{O}_N$ and $\text{K}\cdots\text{O}_N$ contact pair configurations, and (4) the heavy-water NDIS-based water-

hydrogen coordination around the oxygen site of the nitrate ion, $n_D^{\text{O}_N}(r_u)$, appears to provide an adequate measure of the actual due to the absence of any potential overlapping between the first peaks of the $\text{D}\cdots\text{O}_N$ and the $\text{O}_w\cdots\text{O}_N$ pair correlations. Moreover, the water–nitrate coordination suggests that the XRD frequently invoked conjectured relationship $n_{\text{O}_w}^N(r_u) = 3n_{\text{O}_w}^{\text{O}_N}(r_u)$ is not supported by the molecular-based microstructure of the aqueous KNO_3 systems.

Although we studied the solvation behavior of the aqueous nitrate systems based on realistic fixed-charge intermolecular potentials models, we are certainly aware of the fact that water is a polarizable environment,^{97–99} and consequently, the description of some features of the anion hydration behavior might be improved by the use of a model involving induced-dipole polarization. Work toward that end is currently underway.¹⁰⁰

In summary, our analysis supports the theoretical feasibility of performing NDIS experiments involving $^{14}\text{N}/^{15}\text{N}$ and $^{\text{nat}}\text{O}_N/^{18}\text{O}_N$ in heavy- and null-aqueous environments as a means to extract the complete coordination behavior of water around the nitrate ion. The challenge now is for our neutron scattering colleagues to confront the difficulties underlying these NDIS experiments and translate the proposed scheme into a viable tool to provide an accurate characterization of the nitrate hydration, a task that is currently underway.

APPENDIX A: DERIVATION OF THE NDIS EXPRESSION FOR THE DETERMINATION OF THE SECOND COORDINATION NUMBER FOR THE WATER-HYDROGEN SITE AROUND THE NITRATE-NITROGEN SITE

Starting from the expressions 2.7 and 2.8, recalling the meaning of the coefficients, and the fact that the two aqueous solutions must have precisely the same atomic fraction (composition), then

$$\begin{aligned} \Sigma_N^{\text{hw}} \Delta G_N^{\text{hw}, \text{norm}}(r) - \Sigma_N^{\text{nw}} \Delta G_N^{\text{nw}, \text{norm}}(r) \\ = (A_N^{\text{hw}} - A_N^{\text{nw}})g_{\text{ON}_N}(r) + B_N^{\text{hw}}g_{\text{DN}}(r) + (D_N^{\text{hw}} - D_N^{\text{nw}})g_{\text{KN}}(r) \\ + (E_N^{\text{hw}} - E_N^{\text{nw}})g_{\text{NN}}(r) + (F_N^{\text{hw}} - F_N^{\text{nw}})g_{\text{O}_N\text{N}}(r) \end{aligned} \quad (\text{A1})$$

where the four coefficient differences between parentheses are null (see Table 3) so that,

$$\Sigma_N^{\text{hw}} \Delta G_N^{\text{hw}, \text{norm}}(r) - \Sigma_N^{\text{nw}} \Delta G_N^{\text{nw}, \text{norm}}(r) = B_N^{\text{hw}}g_{\text{DN}}(r) \quad (\text{A2})$$

Now, after invoking the definition of the water-hydrogen coordination number around the nitrogen site, *i.e.*,

$$n_D^N(r) = 4\pi\rho_D \int_{r_2}^{r_3} g_{\text{DN}}(r)r^2 dr \quad (\text{A3})$$

and substituting eq A2 into eq A3, we finally have that

$$\begin{aligned} n_D^N(r) \\ = (4\pi\rho_D/B_N^{\text{hw}}) \int_{r_2}^{r_3} [\Sigma_N^{\text{hw}} \Delta G_N^{\text{hw}, \text{norm}}(r) - \Sigma_N^{\text{nw}} \Delta G_N^{\text{nw}, \text{norm}}(r)]r^2 dr \end{aligned} \quad (\text{A4})$$

where r_2 and r_3 are the locations of the minima defining the second peak of the $g_{\text{DN}}(r)$.

APPENDIX B: LINK BETWEEN THE DEGREE OF ION-PAIR ASSOCIATION α_{-+} AND THE ANION–CATION RADIAL DISTRIBUTION FUNCTION $G_{-+}(r)$ FOR A SYMMETRIC ELECTROLYTE⁶⁸

The degree of ion-pair association α_{-+} is defined by the radial integral over the corresponding (to be derived) ion-pair radial distribution function $G_{-+}(r)$, *i.e.*,

$$\alpha_{-+}(d_{-+}) = \int_0^{d_{-+}} G_{-+}(r) dr \quad (B1)$$

under the condition that, in the thermodynamic limit, $\lim_{d_{-+} \rightarrow \infty} \alpha_{-+}(d_{-+}) = 1.0$. Note that $G_{-+}(r)\Delta r$ describes the probability of finding an anion in the spherical shell of thickness Δr , within a distance r from a cation, when neither the anion nor the cation engages in additional pairing within that distance r . Thus, from a statistical mechanical standpoint, $G_{-+}(r)$ can be expressed by the following integral equation,

$$G_{-+}(r) = 4\pi\rho_+ g_{-+}(r)r^2 P_-(r) P_+(r) \quad (B2)$$

i.e., in terms of two (yet to be determined) radial functions $P_-(r)$ and $P_+(r)$, where $P_-(r)$ ($P_+(r)$) describes the probability that an anion (cation) located within a distance r from a cation (anion) does not form ion pairs with any other ion of the opposite charge. In other words,

$$\begin{aligned} P_-(r) &= 1 - \int_0^r G_{-+}(s) ds \\ P_+(r) &= 1 - \int_0^r G_{+-}(s) ds \end{aligned} \quad (B3)$$

In order to solve eqs B2 and B3, we invoke the underlying (species conservation) boundary conditions for a symmetric electrolyte, *i.e.*,

$$\rho_- G_{-+}(r) = \rho_+ G_{+-}(r) \quad (B4)$$

since the condition of electroneutrality requires that $g_{-+}(r) = g_{+-}(r)$.¹⁰¹ Obviously, from eqs B2–B4 we have that $P_-(r) = P_+(r)$ because $\rho_+ = \rho_-$, and therefore the solution of the integral eq B2 becomes

$$P_-(r) = [1 + 4\pi\rho_+ \int_0^r g_{-+}(s)s^2 ds]^{-1} \quad (B5)$$

and, consequently,

$$G_{-+}(r) = 4\pi\rho_+ g_{-+}(r)r^2 / [1 + 4\pi\rho_+ \int_0^r g_{-+}(s)s^2 ds]^2 \quad (B6)$$

In addition, as required by the definition of α_{-+} , $G_{-+}(r)$ given by eq B6 satisfies the normalization condition; *i.e.*,

$$\int_0^\infty G_{-+}(r) dr = 1 - [1 + 4\pi\rho_+ \int_0^\infty g_{-+}(r)r^2 dr]^{-1} = 1 \quad (B7)$$

AUTHOR INFORMATION

Corresponding Author

*E-mail: chialvoaa@ornl.gov. Fax: 865-574-4961.

Notes

The authors declare no competing financial interest.

ACKNOWLEDGMENTS

This work was supported by the U.S. Department of Energy, Office of Science, Office of Basic Energy Sciences, Chemical Sciences, Geosciences, and Biosciences Division.

REFERENCES

- (1) Bickmore, B. R.; Nagy, K. L.; Young, J. S.; Drexler, J. W. Nitrate-Cancrinite Precipitation on Quartz Sand in Simulated Hanford Tank Solutions. *Environ. Sci. Technol.* **2001**, *35*, 4481–4486.
- (2) Wayne, R. P. *Chemistry of Atmospheres: An Introduction to the Chemistry of the Atmospheres of Earth, the Planets, and Their Satellites*; Oxford University Press: Oxford, U.K., 2000.
- (3) Caminiti, R.; Licheri, G.; Paschina, G.; Piccaluga, G.; Pinna, G. Interactions and Structure in Aqueous NaNO_3 Solutions. *J. Chem. Phys.* **1980**, *72*, 4522–4528.
- (4) Caminiti, R.; Licheri, G.; Piccaluga, G.; Pinna, G. On NO_3^- - H_2O Interactions in Aqueous Solutions. *J. Chem. Phys.* **1978**, *68*, 1967–1970.
- (5) Dagnall, S. P.; Hague, D. N.; Towle, A. D. C. X-Ray-Diffraction Study of Aqueous Zinc(II) Nitrate. *J. Chem. Soc., Faraday Trans. 2* **1982**, *78*, 2161–2167.
- (6) Caminiti, R.; Cucca, P.; Radnai, T. Investigation on the Structure of Cadmium Nitrate Aqueous-Solutions by X-ray Diffraction and Raman Spectroscopy. *J. Phys. Chem.* **1984**, *88*, 2382–2386.
- (7) Caminiti, R.; Atzei, D.; Cucca, P.; Anedda, A.; Bongiovanni, G. Structure of Rhodium(III) Nitrate Aqueous-Solutions. An Investigation by X-ray Diffraction and Raman Spectroscopy. *J. Phys. Chem.* **1986**, *90*, 238–243.
- (8) Valeev, A. K.; Smirnov, P. R.; Trostian, V. N.; Krestov, G. A. Characteristics of Nitrate-Ion Hydration in Aqueous-Solutions in Nitric-Acid. *Russ. J. Phys. Chem.* **1988**, *62*, 155–157.
- (9) Burke, C. A. E.; Adya, A. K.; Neilson, G. W. A Structural Study of the Aqua-Anions NO_3^- , BrO_3^- and ClO_3^- by Difference Methods of X-ray Diffraction. *J. Phys.: Condens. Matter* **1991**, *3*, 837–850.
- (10) Smirnov, P.; Yamagami, M.; Wakita, H.; Yamaguchi, T. An X-Ray Diffraction Study on Concentrated Aqueous Calcium Nitrate Solutions at Subzero Temperatures. *J. Mol. Liq.* **1997**, *73–4*, 305–316.
- (11) Marques, M. A.; Marques, M. I. D.; Cabaco, M. I.; Gaspar, A. M.; de Almeida, M. L. Intermediate Range Order in Concentrated Aqueous Solutions of Copper Nitrate. X-Ray Diffraction and Raman Investigations. *J. Mol. Liq.* **2004**, *110*, 23–31.
- (12) Levochkin, S. F.; Smirnov, P. R.; Trostian, V. N. D-Structure of Aqueous Solutions of Cobalt(II) Nitrate at 298 And. 323 K by X-Ray Diffraction. *Russ. J. Gen. Chem.* **2005**, *75*, 1180–1185.
- (13) Cabaco, M. I.; Marques, M. I. D.; Marques, M. A.; Gaspar, A. M.; de Almeida, M. L. X-Ray Diffraction and Raman Spectroscopy Investigations in Concentrated Aqueous Solutions of Yttrium and Strontium Nitrates. *J. Mol. Liq.* **2005**, *117*, 69–76.
- (14) Marques, M. A.; Marques, M. I. D.; Cabaco, M. I.; Gaspar, A. M.; Marques, M. P. M.; Amado, A. M.; da Costa, A. M. A. Evidence of a Local Order in Concentrated Aqueous Solutions of Salts Constituted by Ions of Different Valences. X-Ray Diffraction and Raman Spectroscopy Experiments. *J. Mol. Liq.* **2007**, *134*, 142–150.
- (15) Cabaco, M. I.; Marques, M.; Gaspar, A. M.; Marques, M. A.; Costa, M. M. The Structure of Concentrated Aqueous Solutions of Chromium Nitrate and Cerium Chloride Studied by X-Ray Diffraction and Raman Spectroscopy. *J. Mol. Liq.* **2007**, *136*, 323–330.
- (16) Smirnov, P. R.; Grechin, O. V.; Trostian, V. N. Concentration Dependence of the Structure of Aqueous Solutions of Lutetium Nitrate According to X-Ray Diffraction. *Russ. J. Phys. Chem. A* **2014**, *88*, 250–253.
- (17) Neilson, G. W.; Enderby, J. E. The Structure around Nitrate Ions in Concentrated Aqueous-Solutions. *J. Phys. C: Solid State Phys.* **1982**, *15*, 2347–2352.
- (18) Walker, P. A. M.; Lawrence, D. G.; Neilson, G. W.; Cooper, J. The Structure of Concentrated Aqueous Ammonium-Nitrate Solutions. *J. Chem. Soc., Faraday Trans. 1* **1989**, *85*, 1365–1372.

- (19) Adya, A. K.; Neilson, G. W. Structure of a 50 mol kg⁻¹ Aqueous-Solution of Ammonium-Nitrate at 373-K by the Isotopic Difference Method of Neutron-Diffraction. *J. Chem. Soc., Faraday Trans.* **1991**, *87*, 279–286.
- (20) Kameda, Y.; Saitoh, H.; Uemura, O. The Hydration Structure of NO₃⁻ in Concentrated Aqueous Sodium Nitrate Solutions. *Bull. Chem. Soc. Jpn.* **1993**, *66*, 1919–1923.
- (21) Mason, P. E.; Neilson, G. W.; Dempsey, C. E.; Brady, J. W. Neutron Diffraction and Simulation Studies of CsNO₃ and Cs₂Co₃ Solutions. *J. Am. Chem. Soc.* **2006**, *128*, 15136–15144.
- (22) Megyes, T.; Balint, S.; Peter, E.; Grosz, T.; Bakó, I.; Krienke, H.; Bellissent-Funel, M. C. Solution Structure of NaNO₃ in Water: Diffraction and Molecular Dynamics Simulation Study. *J. Phys. Chem. B* **2009**, *113*, 4054–4064.
- (23) Irish, D. E.; Davis, A. R.; Plane, R. A. Types of Interaction in Some Aqueous Metal Nitrate Systems. *J. Chem. Phys.* **1969**, *50*, No. 2262.
- (24) Irish, D. E.; Chang, G.; Nelson, D. L. Cation-Nitrate Ion Contact in Aqueous Solutions. *Inorg. Chem.* **1970**, *9*, 425–426.
- (25) Vogrin, F. J.; Knapp, P. S.; Flint, W. L.; Anton, A.; Highberger, G.; Malinowski, E. R. NMR Studies of Aqueous Electrolyte Solutions. IV. Hydration Numbers of Strong Electrolytes Determined from Temperature Effects on Proton Shifts. *J. Chem. Phys.* **1971**, *54*, 178–181.
- (26) Chizhik, V. I. NMR Relaxation and Microstructure of Aqueous Electrolyte Solutions. *Mol. Phys.* **1997**, *90*, 653–659.
- (27) Nicholas, A. M. D.; Wasylshen, R. E. A Nuclear-Magnetic-Resonance Study of Aqueous Solutions of Several Nitrate Salts. *Can. J. Chem. (Rev. Can. Chim.)* **1987**, *65*, 951–956.
- (28) Adachi, A.; Kiyoyama, H.; Nakahara, M.; Masuda, Y.; Yamatera, H.; Shimizu, A.; Taniguchi, Y. Raman and Nuclear Magnetic Resonance Studies on the Concentration Dependence of Orientational Relaxation Times of the Nitrate Ion in Dilute Aqueous Solution. *J. Chem. Phys.* **1989**, *90*, 392–399.
- (29) Owens, G.; Guarilloff, P.; Steel, B. J.; Kurucsev, T. N-14 Nuclear-Magnetic-Resonance Relaxation of the Nitrate Ion and Ion-Pairing in Aqueous-Solution. *Aust. J. Chem.* **1995**, *48*, 207–215.
- (30) Vollmar, P. M. Ionic Interactions in Aqueous Solution: A Raman Spectral Study. *J. Chem. Phys.* **1963**, *39*, 2236–2248.
- (31) Peleg, M. Raman Spectroscopic Investigation of Magnesium Nitrate-Water System. *J. Phys. Chem.* **1972**, *76*, 1019–1025.
- (32) Waterland, M. R.; Stockwell, D.; Kelley, A. M. Symmetry Breaking Effects in NO₃⁻: Raman Spectra of Nitrate Salts and ab Initio Resonance Raman Spectra of Nitrate-Water Complexes. *J. Chem. Phys.* **2001**, *114*, 6249–6258.
- (33) Zhang, Y. H.; Choi, M. Y.; Chan, C. K. Relating Hygroscopic Properties of Magnesium Nitrate to the Formation of Contact Ion Pairs. *J. Phys. Chem. A* **2004**, *108*, 1712–1718.
- (34) Rohman, N.; Wahab, A.; Mahiuddin, S. Isentropic Compressibility, Shear Relaxation Time, and Raman Spectra of Aqueous Calcium Nitrate and Cadmium Nitrate Solutions. *J. Solution Chem.* **2005**, *34*, 77–94.
- (35) Choppin, G. R.; Buijs, K. Near-Infrared Studies of Structure of Water 0.2. Ionic Solutions. *J. Chem. Phys.* **1963**, *39*, No. 2042.
- (36) Sze, Y. K.; Irish, D. E. Vibrational Spectral Studies of Ion-Ion and Ion-Solvent Interactions. 1. Zinc Nitrate in Water. *J. Solution Chem.* **1978**, *7*, 395–415.
- (37) Bergstrom, P. A.; Lindgren, J.; Kristiansson, O. An IR Study of the Hydration of Perchlorate, Nitrate, Iodide, Bromide, Chloride, and Sulfate Anions in Aqueous Solution. *J. Phys. Chem.* **1991**, *95*, 8575–8580.
- (38) Liu, J. H.; Zhang, Y. H.; Wang, L. Y.; Wei, Z. F. Drawing out the Structural Information of the First Layer of Hydrated Ions: ATR-FTIR Spectroscopic Studies on Aqueous NH₄NO₃, NaNO₃, and Mg(NO₃)₂ Solutions. *Spectrochim. Acta, Part A* **2005**, *61*, 893–899.
- (39) Goebbert, D. J.; Garand, E.; Wende, T.; Bergmann, R.; Meijer, G.; Asmis, K. R.; Neumark, D. M. Infrared Spectroscopy of the Microhydrated Nitrate Ions NO₃⁻(H₂O)_{1–6}. *J. Phys. Chem. A* **2009**, *113*, 7584–7592.
- (40) Shaffer, C. J.; Schroder, D. Microhydrated Cobalt-Nitrate Cations Co(NO₃)(H₂O)(N) (+) (N=2, 3) Studied by Infrared Spectroscopy in the Gas Phase. *Int. J. Mass Spectrom.* **2012**, *311*, 17–23.
- (41) Fleissner, G.; Hallbrucker, A.; Mayer, E. Nu(2) Band Region of Nitrate as an Indicator for Contact Ion Pairing in Aqueous Lithium and Calcium Nitrate Solutions. *J. Chem. Soc., Faraday Trans.* **1996**, *92*, 23–28.
- (42) Howell, J. M.; Sapce, A. M.; Singman, E.; Synder, G. Ab Initio SCF Calculations of NO₂-(H₂O)_n and NO₃-(H₂O)_n Clusters. *J. Phys. Chem.* **1982**, *86*, 2345–2349.
- (43) Shen, M. Z.; Xie, Y. M.; Schaefer, H. F.; Deakyne, C. A. Hydrogen-Bonding between the Nitrate Anion (Conventional and Peroxy Forms) and the Water Molecule. *J. Chem. Phys.* **1990**, *93*, 3379–3388.
- (44) Ebner, C.; Sansone, R.; Probst, M. Quantum Chemical Study of the Interaction of Nitrate Anion with Water. *Int. J. Quantum Chem.* **1998**, *70*, 877–886.
- (45) Dobler, M.; Guilbaud, P.; Dedieu, A.; Wipff, G. Interaction of Trivalent Lanthanide Cations with Nitrate Anions: A Quantum Chemical Investigation of Monodentate/Bidentate Binding Modes. *New J. Chem.* **2001**, *25*, 1458–1465.
- (46) Lebrero, M. C. G.; Bikiel, D. E.; Elola, M. D.; Estrin, D. A.; Roitberg, A. E. Solvent-Induced Symmetry Breaking of Nitrate Ion in Aqueous Clusters: A Quantum-Classical Simulation Study. *J. Chem. Phys.* **2002**, *117*, 2718–2725.
- (47) Tongraar, A.; Tangkawanwanit, P.; Rode, B. M. A Combined QM/MM Molecular Dynamics Simulations Study of Nitrate Anion (NO₃⁻) in Aqueous Solution. *J. Phys. Chem. A* **2006**, *110*, 12918–12926.
- (48) Ramesh, S. G.; Re, S. Y.; Hynes, J. T. Charge Transfer and Oh Vibrational Frequency Red Shifts in Nitrate-Water Clusters. *J. Phys. Chem. A* **2008**, *112*, 3391–3398.
- (49) Zhang, H.; Zhang, Y. H. Ab Initio Investigation on the Ion-Associated Species and Process in Mg(NO₃)₂ Solution. *J. Comput. Chem.* **2010**, *31*, 2772–2782.
- (50) Pathak, A. K. Theoretical Study on Microhydration of NO₃-Ion: Structure and Polarizability. *Chem. Phys.* **2011**, *384*, 52–56.
- (51) Kataoka, Y. Molecular-Dynamics Simulation of Aqueous MnO₃ (M = Li, Na, K, Rb, and Cs) Solutions. *Bull. Chem. Soc. Jpn.* **1993**, *66*, 2478–2491.
- (52) Ebner, C.; Sansone, R.; Hengrasme, S.; Probst, M. Molecular Dynamics Study of an Aqueous Potassium Nitrate Solution. *Int. J. Quantum Chem.* **1999**, *75*, 805–814.
- (53) Lu, G. W.; Li, C. X.; Wang, W. C.; Wang, Z. H. A Monte Carlo Simulation on Structure and Thermodynamics of Potassium Nitrate Electrolyte Solution. *Mol. Phys.* **2005**, *103*, 599–610.
- (54) Dang, L. X.; Chang, T. M.; Roeselova, M.; Garrett, B. C.; Tobias, D. J., On NO₃⁻-H₂O Interactions in Aqueous Solutions and at Interfaces. *J. Chem. Phys.* **2006**, *124*.
- (55) Krienke, H.; Opalka, D. Hydration of Molecular Ions: A Molecular Dynamics Study with a SPC/E Water Model. *J. Phys. Chem. C* **2007**, *111*, 15935–15941.
- (56) Xu, M.; Larentzos, J. P.; Roshdy, M.; Criscenti, L. J.; Allen, H. C. Aqueous Divalent Metal-Nitrate Interactions: Hydration Versus Ion Pairing. *Phys. Chem. Chem. Phys.* **2008**, *10*, 4793–4801.
- (57) Miller, Y.; Thomas, J. L.; Kemp, D. D.; Finlayson-Pitts, B. J.; Gordon, M. S.; Tobias, D. J.; Gerber, R. B. Structure of Large Nitrate-Water Clusters at Ambient Temperatures: Simulations with Effective Fragment Potentials and Force Fields with Implications for Atmospheric Chemistry. *J. Phys. Chem. A* **2009**, *113*, 12805–12814.
- (58) Duvail, M.; Guilbaud, P. Understanding the Nitrate Coordination to Eu(3+) Ions in Solution by Potential of Mean Force Calculations. *Phys. Chem. Chem. Phys.* **2011**, *13*, 5840–5847.
- (59) Vchirawongkwin, V.; Kritayakornupong, C.; Tongraar, A.; Rode, B. M. Symmetry Breaking and Hydration Structure of Carbonate and Nitrate in Aqueous Solutions: A Study by ab Initio Quantum Mechanical Charge Field Molecular Dynamics. *J. Phys. Chem. B* **2011**, *115*, 12527–12536.

- (60) Averina, M. I.; Egorov, A. V.; Chizhik, V. I. Microstructure of Concentrated Solutions in the Water-Lithium Nitrate-Calcium Nitrate Ternary System from Molecular Dynamics Simulations. *J. Struct. Chem.* **2013**, *54*, 289–296.
- (61) Richens, D. T. *Chemistry of Aqua Ions*; Wiley: Chichester, U.K., 1997.
- (62) Fischer, H. E.; Simonson, J. M.; Neufeind, J. C.; Lemmel, H.; Rauch, H.; Zeidler, A.; Salmon, P. S. The Bound Coherent Neutron Scattering Lengths of the Oxygen Isotopes. *J. Phys.: Condens. Matter* **2012**, *24*, 24505105.
- (63) Sears, V. F. Feature Section of Neutron Scattering Lengths and Cross Sections of the Elements and Their Isotopes. *Neutron News* **1992**, *3*, 29–37.
- (64) Zeidler, A.; Salmon, P. S.; Fischer, H. E.; Neufeind, J. C.; Simonson, J. M.; Markland, T. E. Isotope Effects in Water as Investigated by Neutron Diffraction and Path Integral Molecular Dynamics. *J. Phys.: Condens. Matter* **2012**, *24*, 24284126.
- (65) Chialvo, A. A.; Simonson, J. M. The Structure of Concentrated NiCl_2 Aqueous Solutions. What Is Molecular Simulation Revealing About the Neutron Scattering Methodologies? *Mol. Phys.* **2002**, *100*, 2307–2315.
- (66) Chialvo, A. A.; Simonson, J. M. The Structure of CaCl_2 Aqueous Solutions over a Wide Range of Concentrations. Interpretation of Diffraction Experiments Via Molecular Simulation. *J. Chem. Phys.* **2003**, *119*, 8052–8061.
- (67) Chialvo, A. A.; Simonson, J. M. Ion Association in Aqueous LiCl Solutions at High Concentration: Predicted Results Via Molecular Simulation. *J. Chem. Phys.* **2006**, *124*, 154509.
- (68) Poirier, J. C.; DeLap, J. H. On the Theory of Ion Pairs in Solutions. *J. Chem. Phys.* **1961**, *35*, 213–227.
- (69) Enderby, J. E. Ion Solvation Via Neutron Scattering. *Chem. Soc. Rev.* **1995**, *24*, 159–168.
- (70) Neilson, G. W.; Mason, P. E.; Ramos, S.; Sullivan, D. Neutron and X-Ray Scattering Studies of Hydration in Aqueous Solutions. *Philos. Trans. R. Soc., A* **2001**, *359*, 1575–1591.
- (71) Ansell, S.; Barnes, A. C.; Mason, P. E.; Neilson, G. W.; Ramos, S. X-Ray and Neutron Scattering Studies of the Hydration Structure of Alkali Ions in Concentrated Aqueous Solutions. *Biophys. Chem.* **2006**, *124*, 171–179.
- (72) Badyal, Y. S.; Barnes, A. C.; Cuello, G. J.; Simonson, J. M. Understanding the Effects of Concentration on the Solvation Structure of Ca^{2+} in Aqueous Solutions. II: Insights into Longer Range Order from Neutron Diffraction Isotope Substitution. *J. Phys. Chem. A* **2004**, *108*, 11819–11827.
- (73) Fulton, J. L.; Heald, S. M.; Badyal, Y. S.; Simonson, J. M. Understanding the Effects of Concentration on the Solvation Structure of Ca^{2+} in Aqueous Solution. I: The Perspective on Local Structure from EXAFS and XANES. *J. Phys. Chem. A* **2003**, *107*, 4688–4696.
- (74) Price, D. L.; Pasquarello, A. Number of Independent Partial Structure Factors for a Disordered N-Component System. *Phys. Rev. B* **1999**, *59*, 5–7.
- (75) Soper, A. K.; Neilson, G. W.; Enderby, J. E. Neutron Diffraction Study of Hydration Effects in Aqueous Solutions. *J. Phys. C: Solid State Phys.* **1977**, *10*, 1793–1801.
- (76) Placzek, G. The Scattering of Neutrons by Systems of Heavy Nuclei. *Phys. Rev.* **1952**, *86*, 377–388.
- (77) Soper, A. K. The Radial Distribution Functions of Water as Derived from Radiation Total Scattering Experiments: Is There Anything We Can Say for Sure? *ISRN Phys. Chem.* **2013**, *2013*, 67.
- (78) Powell, D. H.; Neilson, G. W.; Enderby, J. E. A Neutron Diffraction Study of NiCl_2 in D_2O and H_2O . A Direct Determination of $G_{\text{nh}}(\text{R})$. *J. Phys.: Condens. Matter* **1989**, *1*, 8721–8733.
- (79) Lee, H.; Wilmhurst, J. K. Observation of Ion-Pairs in Aqueous Solutions by Vibrational Spectroscopy. *Aust. J. Chem.* **1964**, *17*, 943–945.
- (80) Irish, D. E.; Davis, A. R. Interactions in Aqueous Alkali Metal Nitrate Solutions. *Can. J. Chem.* **1968**, *46*, 943–951.
- (81) Riddell, J. D.; Irish, D. E.; Lockwood, D. J. Ion-Pair Formation in $\text{NaNO}_3/\text{D}_2\text{O}$ Solution: Raman and Infrared Spectra, Partial Molal Volumes, Conductance, and Viscosity. *Can. J. Chem.* **1972**, *50*, 2951–&.
- (82) Hester, R. E.; Plane, R. A. Vibrational Spectroscopic Study of Contact Ion Pairing between Zn^{++} and NO_3^- in Water. *J. Chem. Phys.* **1966**, *45*, 4588–4593.
- (83) Frost, R. L.; James, D. W. Ion Ion Solvent Interactions in Solution. 3. Aqueous-Solutions of Sodium-Nitrate. *J. Chem. Soc., Faraday Trans. 1* **1982**, *78*, 3223–3234.
- (84) James, D. W.; Frost, R. L. Ion Ion Solvent Interactions in Solution—Aqueous-Solutions of Nitrates of Cations from Group-2a and Group-3a. *Aust. J. Chem.* **1982**, *35*, 1793–1806.
- (85) Berendsen, H. J. C.; Grigera, J. R.; Straatsma, T. P. The Missing Term in Effective Pair Potentials. *J. Phys. Chem.* **1987**, *91*, 6269–6271.
- (86) Dang, L. X. Mechanism and Thermodynamics of Ion Selectivity in Aqueous Solutions of 18-Crown-6 Ether: A Molecular Dynamics Study. *J. Am. Chem. Soc.* **1995**, *117*, 6954–6960.
- (87) Nose, S. An Improved Symplectic Integrator for Nose-Poincare Thermostat. *J. Phys. Soc. Jpn.* **2001**, *70*, 75–77.
- (88) Okumura, H.; Itoh, S. G.; Okamoto, Y. Explicit Symplectic Integrators of Molecular Dynamics Algorithms for Rigid-Body Molecules in the Canonical, Isobaric-Isothermal, and Related Ensembles. *J. Chem. Phys.* **2007**, *126*, No. 084103.
- (89) Martinez, J. M.; Martinez, L. Packing Optimization for Automated Generation of Complex System's Initial Configurations for Molecular Dynamics and Docking. *J. Comput. Chem.* **2003**, *24*, 819–825.
- (90) Fincham, D. Optimization of the Ewald Sum for Large Systems. *Mol. Simul.* **1994**, *13*, 1–9.
- (91) Chialvo, A. A.; Cummings, P. T. Microstructure of Ambient and Supercritical Water. A Direct Comparison between Simulation and Neutron Scattering Experiments. *J. Phys. Chem.* **1996**, *100*, 1309–1316.
- (92) Caminiti, R.; Cucca, P.; Dandrea, A. Hydration Phenomena in a Concentrated Aqueous-Solution of $\text{Ce}(\text{NO}_3)_3$ —X-Ray-Diffraction and Raman-Spectroscopy. *Z. Naturforsch., A: Phys. Sci.* **1983**, *38*, 533–539.
- (93) Caminiti, R.; Cucca, P.; Pintori, T. Hydration and Ion-Pairing in Concentrated Aqueous $\text{Mn}(\text{NO}_3)_2$ Solutions. An X-ray and Raman-Spectroscopy Study. *Chem. Phys.* **1984**, *88*, 155–161.
- (94) Caminiti, R.; Radnai, T. X-Ray-Diffraction Study of a Concentrated $\text{Al}(\text{NO}_3)_3$ Solution. *Z. Naturforsch., A: Phys. Sci.* **1980**, *35*, 1368–1372.
- (95) Kusalik, P. G.; Laaksonen, A.; Svishchev, I. M. Spatial Structure in Molecular Liquids. In *Molecular Dynamics. From Classical to Quantum Methods*; Balbuena, P. B., Seminario, J. M., Eds.; Elsevier: Amsterdam, 1999; pp 61–98.
- (96) Note that under this definition the spatial distribution function is not defined at $\theta = 2n\pi$ since $\sin(2n\pi) = 0$.
- (97) Chialvo, A. A.; Cummings, P. T. Molecular-Based Modeling of Water and Aqueous Solutions at Supercritical Conditions. In *Advances in Chemical Physics*; Rice, S. A., Ed.; John Wiley & Sons: New York, 1999; Vol. 109, pp 115–205.
- (98) Chialvo, A. A.; Horita, J. Polarization Behavior of Water in Extreme Aqueous Environments: A Molecular Dynamics Study Based on the Gaussian Charge Polarizable Water Model. *J. Chem. Phys.* **2010**, *133*.
- (99) Chialvo, A. A.; Vlcek, L. Ewald Summation Approach to Potential Models of Aqueous Electrolytes Involving Gaussian Charges and Induced Dipoles: Formal and Simulation Results. *J. Phys. Chem. B* **2014**, *118*, 13658–13670.
- (100) Vlcek, L.; Uhlik, F.; Moucka, F.; Nezbeda, I.; Chialvo, A. A. Thermodynamics of Small Alkali Halide Cluster Ions: Comparison of Classical Molecular Simulations with Experiment and Quantum Chemistry. *J. Phys. Chem. A* **2014** 10.1021/jp509401d.
- (101) Hansen, J. P.; McDonald, I. R. *Theory of Simple Liquids*, 2nd ed.; Academic Press: New York, 1986.